Screen candidate CO2 sorbent (carrier materials)

CCUS Innovation 2.0

Key Knowledge Deliverable 1.6

October 2024

Contents

Work Package 1.1 – Select 10 candidate inorganic precursors based on results of feasibility studies

The 10 candidate inorganic precursors were identified and investigated based on literature feasibility studies, falling under the described categories. During our investigations, several carrier precursors were identified under each class and are detailed on page 9. The 3 most successful carrier precursors were selected according to their accessibility, CO2 capture potential and following from this study will be developed and investigated for application in transferring CO2 to cementitious materials.

Selection criteria of materials

Given the very specific usage of CO2 sorbent materials: literature investigations and carrier precursor selections were carried out according to two major criteria:

- Cost-effectiveness/abundance.

To be scalable to fit the use within cementitious materials, the raw materials for the carriers must be cost-effective and producible from abundant materials. Use of low abundancy elements (such as rare metal oxides), or materials only producible in small-scales were discounted. Where possible, mass-produced base or starting materials were chosen.

- Mechanism of CO2 sorption

To be suitable for application within cement CO2 sorption is to be targeted through the formation of ‘strong’ bonds. In effect, chemi- as opposed to physisorption is required to provide a delivery mechanism which allows for the potential for a slow CO2 delivery rate in a cementitious environment.

Adsorption profiles of materials

As all sorbents investigated are highly novel, specific CO2 adsorption profiles were measured during the course of this study and summarised in Table 1.

Table 1: Adsorption profiles of materials investigated in this study

Materials	Adsorption profile figure(s)	Page
Silica 1 Amine 1	Figure 12	20
Silica 5 Amine 1	Figure 13	22
Silica 1 Amine 2	Figure 15	25
Silica 2 Amine 2	Figure 14	24
Amine incorporated silicas	Figure 16	25
Amine grafted silicas	Figure 17	27
Amine incorporated polymers	Figure 18	30
Amine incorporated polymers-amine 1	Figure 19	30
Amine incorporated polymers-amine 2	Figure 19	30
Amine 3-liq	Figure 21	34
Amine 3-amine 2	Figure 21	34

Nitrogenous modified solid porous particles

Nitrogen yielding porous structures derivatives exhibiting surface functional groups were identified based on literature feasibility studies as ideal carrier precursor species. CO2 capture by nitrogen enhancement occurs through the formation of salts, which depend on the humidity, pH and temperature.[1],[2],[3] Through this chemisorption process; CO2 sequestration is highly selective and thermodynamically favourable, ideal for the purpose of introducing CO2 into cementitious materials as per the goals of this project.[4]

Figure 1: Structures of Bicarbonate, carbonate, and carbamates

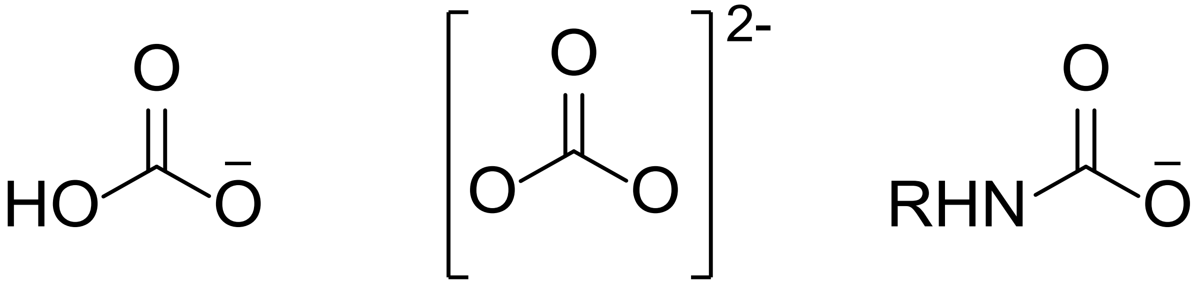

Through the incorporation of a mesoporous solid support, either through impregnation, direct incorporation or surface grafting, the leachability of nitrogen species and environmental impact and the impact on cement setting can be reduced. An abundant, cheap, and easily modified inorganic solid support was identified to be mesoporous materials, which has been used extensively in the field of CO2 capture.[5][6][7] Through the use of a porous substrate, the effective surface area for CO2 capture can be increased, thus facilitating the CO2 capture by the composite materials. From these three categories of nitrogen-modified silicas were fully investigated: nitrogenous impregnated silicas, incorporating silicas, and grafted silicas, with several carrier precursor candidates being studied within each class. This combinatorial approach was undertaken to mitigate risks: each class exhibits advantages and disadvantages which necessitate the multi-branched research strategy.

Nitrogenous impregnated silicas

Impregnation of the porous substrates materials are a process whereby the respective chemicals are introduced through slow perfusion in the porous network via mixing along with a volatile solvent followed by drying. Nitrogenous loading at different levels with respect to the solid support can be modulated to attune CO2 capacities and porosities. silica 1 and silica 5 were selected for this study. An initial investigation into the surface properties was conducted. Both silicas were then impregnated with Amine 1 and Amine 2 at various amine loadings. Scale-up of the impregnation reaction was conducted to a 100g scale. silica 1 and Silica 5 was chosen as a moderate surface-area very cost effective and scalable silica source for surface

---

[1] B. Dutcher, M. Fan and A. G. Russell, ACS Appl Mater Interfaces, 2015, 7, 2137–2148.

[2] T. Čendak, L. Sequeira, M. Sardo, A. Valente, M. L. Pinto and L. Mafra, Chemistry - A European Journal, 2018, 24, 10136–10145.ss

[3] L. Mafra, T. Čendak, S. Schneider, P. V. Wiper, J. Pires, J. R. B. Gomes and M. L. Pinto, J Am Chem Soc, 2017, 139, 389–408.

[4] R. Ben Said, J. M. Kolle, K. Essalah, B. Tangour and A. Sayari, ACS Omega, 2020, 5, 26125–26133.

[5] F. Bai, X. Liu, S. Sani, Y. Liu, W. Guo and C. Sun, Sep Purif Technol, , DOI:10.1016/j.seppur.2022.121539

[6] M. W. Hahn, J. Jelic, E. Berger, K. Reuter, A. Jentys and J. A. Lercher, Journal of Physical Chemistry B, 2016, 120, 1988–1995

[7] N. Hedin and Z. Bacsik, Curr Opin Green Sustain Chem, 2019, 16, 13–19

modification. Without amine modification, fumed silica is known to exhibit completely negligible CO2 sorption.[8]

Amine incorporated silicas

Silica nanoparticles were produced in the hydrolytic sol-gel reaction with differing amine loading levels through stoichiometric control of the reaction mixture. Again, from the literature it can be clearly demonstrated that without amine incorporation, pure silica produced through this methodology absorbs almost no (<1% CO2). Adsorption profiles for the as produced materials have been detailed in the relevant section.

Amine grafted silicas

Amine functionality was incorporated to a silica at different surface loadings to achieve the group of surface-grafted mesoporous silicas.

Nitrogen-rich porous polymeric materials

Nitrogen-rich porous organic polymers (POPs) have proven to have great potential for applications in carbon dioxide capture.[9][10][11][12][13][14] This is attributed to their large surface area, suitable pore size distribution and have suitable interactions with carbon dioxide. A wide range of porous materials has been reported in the literature and shows various carbon dioxide capabilities under various conditions. The interactions of these materials with carbon dioxide can be classified as i) physical adsorption ii) chemical adsorption. In the case of chemical interactions, acid-base neutralization is the most common because the carbon dioxide is acidic and if basic sites are present in the porous material, then this interaction will be possible. In addition to this, dipole-quadrupole interactions are also possible in these systems is the porous material is functionalised with polar groups and these leads to high carbon dioxide capture capacities.

---

[8] B. Yoosuk, T. Wongsanga and P. Prasassarakich, Fuel, 2016, 168, 47–53ss

[9] J. Byun, S. H. Je, H. A. Patel, A. Coskun and C. T. Yavuz, J Mater Chem A Mater, 2014, 2, 12507–12512

[10] T. Islamoğlu, M. Gulam Rabbani and H. M. El-Kaderi, J Mater Chem A Mater, 2013, 1, 10259–10266

[11] T. Tozawa, J. T. A. Jones, S. I. Swamy, S. Jiang, D. J. Adams, S. Shakespeare, R. Clowes, D. Bradshaw, T. Hasell, S. Y. Chong, C. Tang, S. Thompson, J. Parker, A. Trewin, J. Bacsa, A. M. Z. Slawin, A. Steiner and A. I. Cooper, Nat Mater, 2009, 8, 973–978

[12] L. Zou, Y. Sun, S. Che, X. Yang, X. Wang, M. Bosch, Q. Wang, H. Li, M. Smith, S. Yuan, Z. Perry and H. C. Zhou, Advanced Materials, 2017, 29

[13] H. Zeng, X. Qu, D. Xu and Y. Luo, Front Chem, 2022, 10

[14] Y. H. Abdelmoaty, T. D. Tessema, F. A. Choudhury, O. M. El-Kadri and H. M. El-Kaderi, ACS Appl Mater Interfaces, 2018, 10, 16049–16058

Amine 3 inspired materials

Amine 3 has been used in many organic reactions due to its strong alkaline nature. It has high affinities for protons. Therefore, proton acceptors such as Amine 3, can provide a thermodynamic driving force for CO2 capture based on the anion and CO2.

Carbon capture based on chemisorption can be conducted using a combination of amines. In such a reaction, Amine 3 (acts as a Bronsted base) deprotonates the amine, followed by the reaction of CO2 with the alkyl amine (Lewis base, CO2 acceptor) resulting in the formation of a carbamate-based organic salt (mixed carbamate).

Work Package 1.2 – Preparation of 10 inorganic sorbents as porous granulated materials for CO2 adsorption

Justification of the choice of these materials can be found in section 4 of this report.

Figure 2: full collection of all samples produced in this project

Work Package 1.3 – Materials properties characterisation

Given the very broad range of materials produced, characterisation methodologies were prescribed on a case-by-case basis depending on the material composition and changes effected through enhancements where appropriate. The specific characterisation techniques are described below in Table 2. BET was employed where appropriate (see table).

Table 2. Characterisation techniques utilized.

Technique	What is observed	Where appropriate
FTIR (ATR and DRIFTS)	Surface/bulk chemistry (chemical bonding).	Surface modification of materials, reaction verification. Surface properties evaluation
TGA (Programmed decomposition)	Surface loading of functional elements, decomposition profiles	Surface modification of materials, molar loading calculations. Surface content evaluation
Gas sorption analysis (BET)	Surface area and pore distribution	Porous materials, surface area analysis
1H NMR	Characterisation of chemical structure and arrangement in soluble organic small molecule compounds	Ionic liquid calculation

Characterisation of amine impregnated silicas

The silicas used for the preparation of the materials were obtained externally (Silica 1 and silica 5). The properties of the respective silicas are summarised in Table 3.

Table 3. Physical properties of silica 1.

	Silica 1	Silica 5
BET Surface areas (m2/g)	175–225	380
Tamped density (g/L)	40	50
pH	3.8–4.3	3.7-4.3
Loss on drying (%)	<1.5	<1.5
SiO2 Content (%)	>99.8	>99.8
Average particle size (micron)		0.2-0.3

Once impregnated by amines, the silicas characterized by TGA to confirm their amine-loading.

Figure 3: TGA traced thermal decomposition curves (and their first differential) of Silica 1 – amine 2 50% (left) and Silica 5 – amine 1 50% (right).

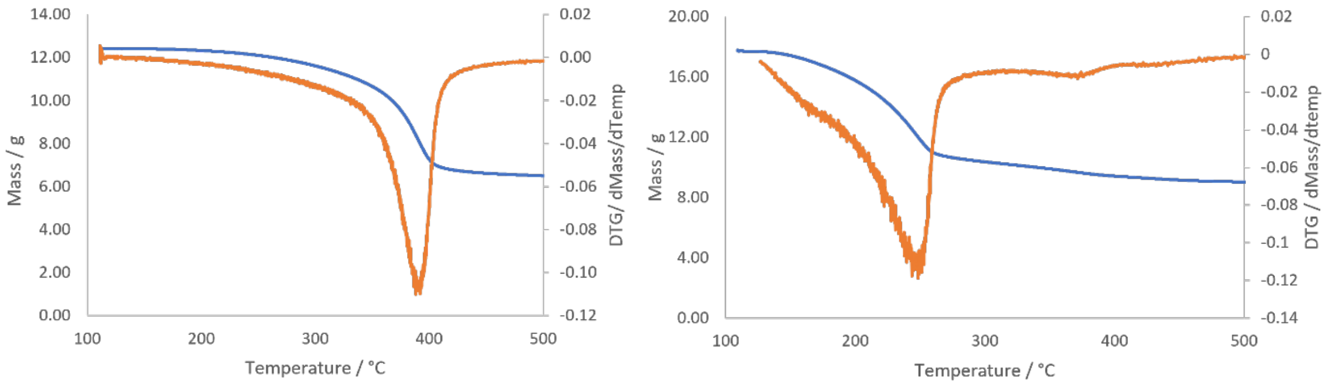

FTIR investigations confirmed the presence of the Amine 2 and Amine 1 in the respective amine samples, with exemplar spectra shown in Figure 4. The silica Si-O-Si asymmetric and symmetric stretches at 1030 and ~800 cm-1 are highly prominent (representing the silica support), with N-H and C-H stretches centred around 3300, 2950 and 2840 cm-1 respectively observed over a broad -OH stretch observable (ascribed to bound water). Alongside C-N stretches and a variety of bending vibrations observable between 1200-1600 cm-1 FTIR spectroscopy confirms the formation of the amine impregnated silica species and the retention of their activity.

Figure 4: FTIR spectra of Silica1- Amine 150% and Silica 1 – amine 1 50%

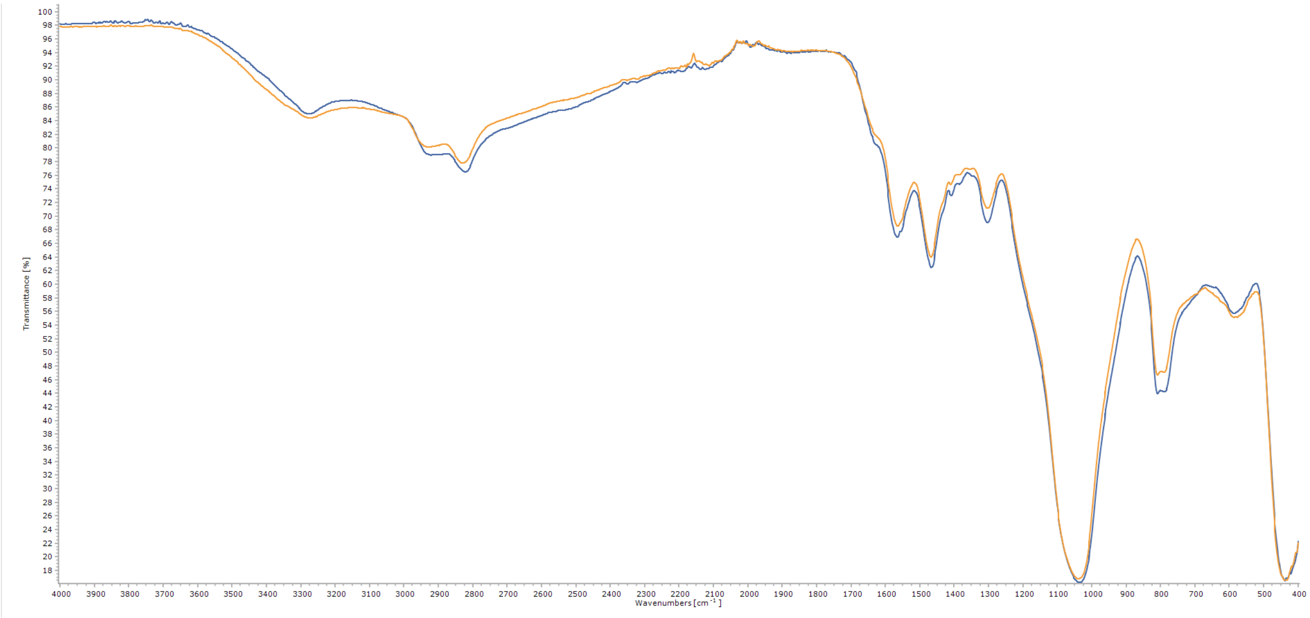

Characterisation of Amine incorporated silicas

The sol-gel produced silicas CSiSG1-3 demonstrated Amine 3 loadings (measured as in section 6.2) in-line with that expected from the concentration in the sol-gel reaction. In all cases amine 2 surface loadings were moderate (Table 9): with a fairly small difference in loading observed across the carrier series despite a large difference in amount of amine 3 available. This suggests that the loading of silica particles produced in this manner is limited by other factors during the sol-gel reaction, which is beyond the scope at this stage of the investigation, however will be studied in future. In all cases, biphasic decomposition profiles reveal a potentially multimodal binding of the amine 3 to the silica surface: however, the predominance of degradation at higher temperatures suggest majority of fully bound species. In comparison with the amine 3 grafted species: loadings of the functional amine species were significantly lower; but degradation was observed at higher temperatures suggesting a more robust binding to the silica surface. When considering the synthesis of these species from the ‘ground-up’, as opposed to simple surface grafting, the more robust inclusion is in line with expectations and demonstrates the value of maintaining the differing approaches.

Figure 5: TGA traced thermal decomposition curves (and their first differential) of CSiG1 (orange solid line), CSiG2 (blue solid line), and CSiG3 (yellow solid line).

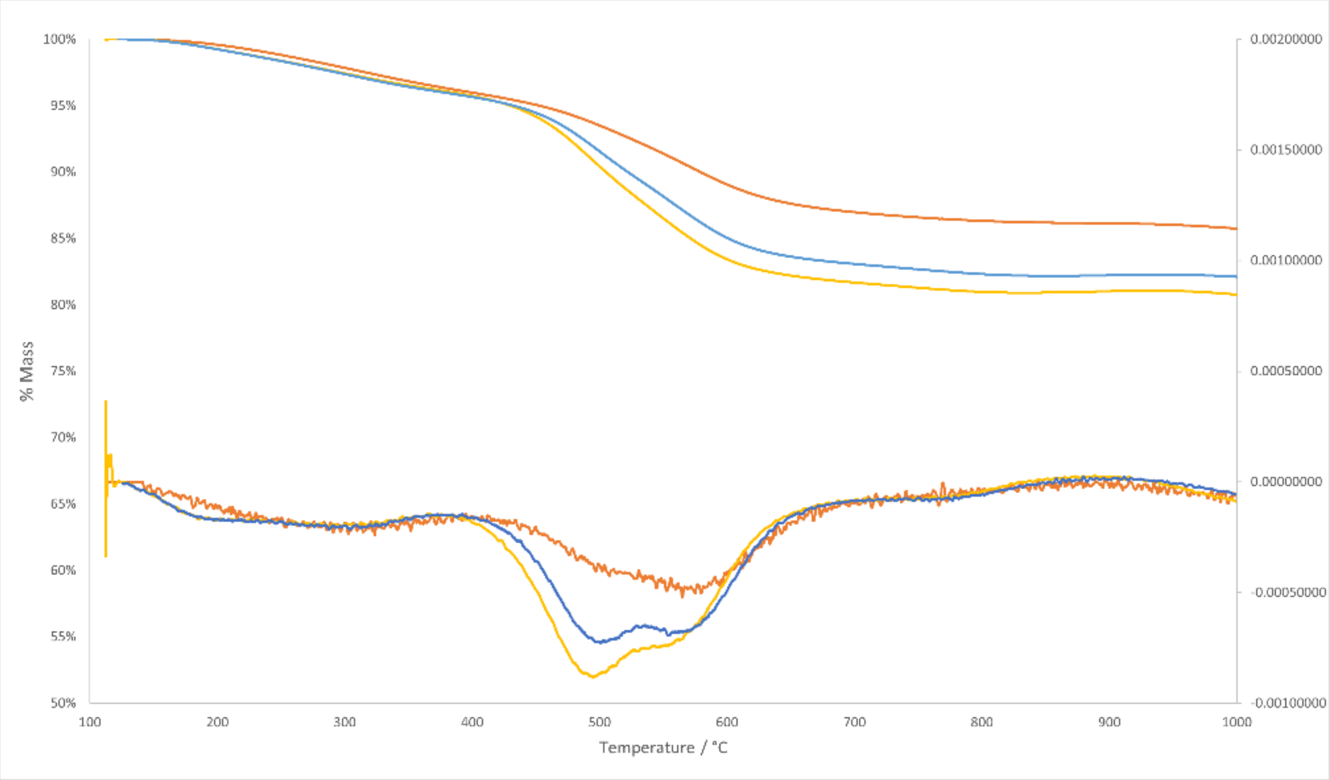

FTIR analysis was performed on the highest-loading condition (CSiG3, Figure 6), as at the time access to FTIR analysis was limited. As for the surface grafted species characterised in section 6.1, the presence of the aminopropyl functional subunit is confirmed by appropriate N-H stretches around 3700 cm-1, C-H stretches around 2700-3000 cm-1, in comparison to the Si-O-Si signals observable at 1070 and 795 cm-1.

Figure 6. FT-IR spectrum for CSiG3

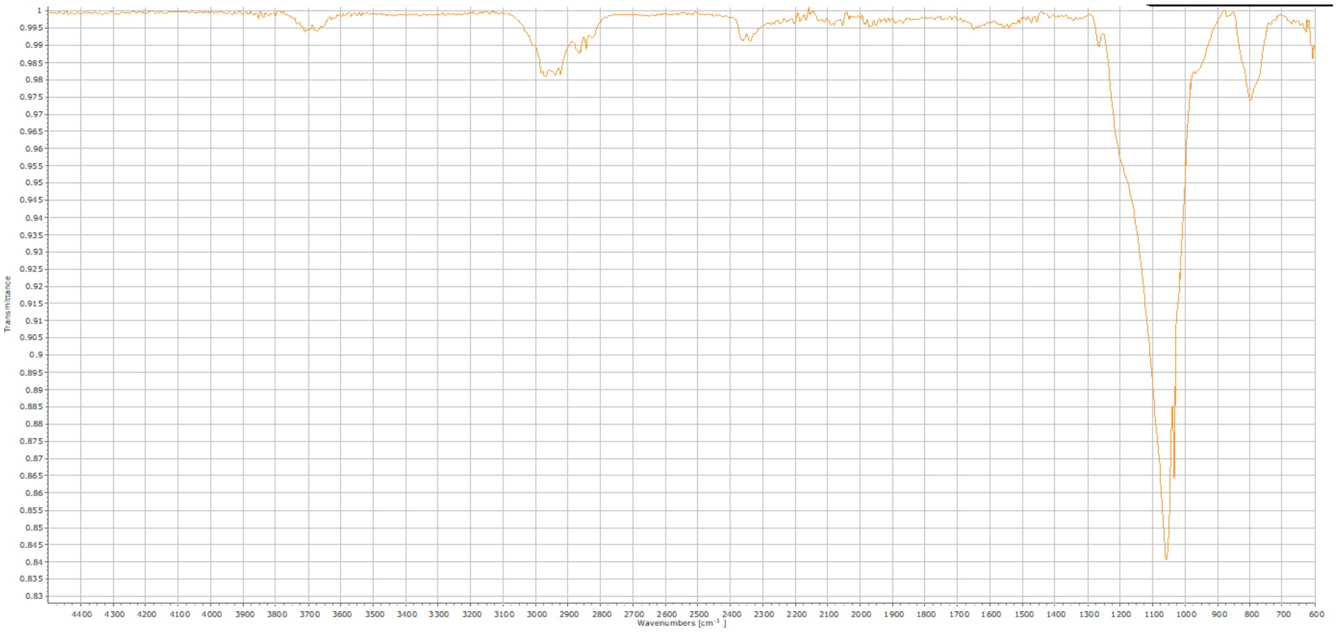

Characterisation of amine grafted silicas

Following the amine grafting reaction, the respective carrier candidates were characterised according to thermal decomposition thermogravimetric analysis under N2 (Table 10, for surface loading characterisation and properties of the Amine 3/SiO2 surface interaction) and infra-red spectroscopic analysis of the produced surface chemistry (Figure 7). Surface area and pore-volume was also calculated according to gas sorption experiments supported by BET calculations.

Silica 1 exhibits almost no appreciable (<1%) thermal degradation under the conditions evaluated during the thermal degradation experiment, allowing us to observe the surface ‘volatile’ content, i.e. the hydrocarbon-amine functionality imparted from the grafting reaction. The mass loss, particularly between 200-800°C is diagnostic of the surface loadings, which can be translated into molar loadings (mMol g-1) when considering the molar mass of the surface-ligated propylamine species. From these results, we clearly demonstrate the ability to control the grafting surface loading through modulating the the grafting parameters. As the surface-grafting of the Amine 3 species to the silica surface is reversible, from a mechanistic point of view for this reaction this observation is in line with expectations

Figure 7: Thermogravimetric decomposition traces (top curves, left axis) and differentiated curves (bottom traces, right axis) of CSiAmG1 (blue), CSiAmG2 (orange), CSiAmG3 (red) and CSiAmG4 (green)

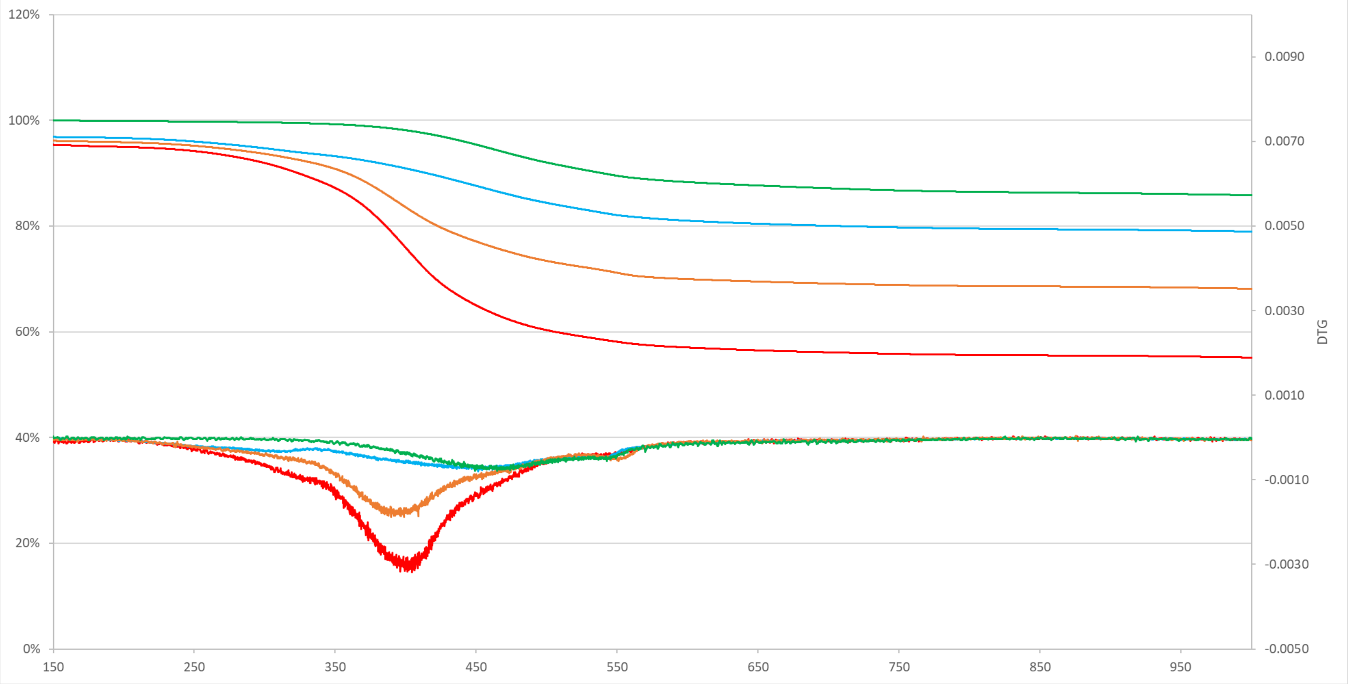

FTIR spectra (Figure 8) demonstrate the consistent surface chemistries of CSiAmG2, CSiAmG3 and CSiAmG4 . Strong resonances originating from symmetric and asymmetric stretches of the Si-O-Si from the silica 1 matrix were consistently observed around 800 cm-1 and 1060 cm-1. The alkylamine surface functionality can be clearly demonstrated by N-H stretching resonances over 3650 cm-1, with C-H stretches observed around 2700-3000 cm-1.

C-N stretching resonances can be observed along with other C-H vibrations around 1300-1700 cm-1. In combination with the decomposition profiles observed in TGA experiments, the FTIR spectra confirm the grafting of the amine functional species to the silica surface. More in depth characterisation of these species is to follow in successive studies, but the surface grafting observed was extremely efficient and reproducible, further supporting the use of these species as carrier candidates.

Figure 8: FTIR spectra of CSiAMG2 (grey), CSiAMG2 (Blue) and CSiAMG4 (orange).

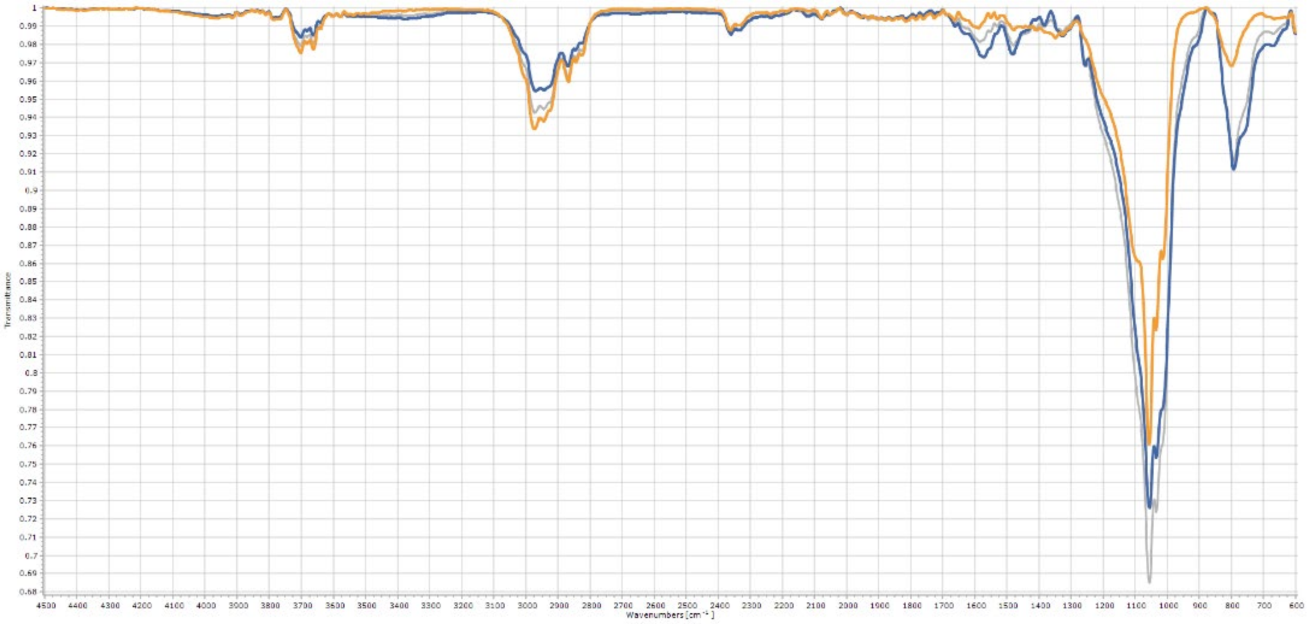

BET evaluation of surface area and porosity was performed on the parent silica 1 and CSiAmG2 as an exemplar comparison of the effect of surface grafting on the silica 1 porosity (Table 4). There is a clear reduction in pore volume and surface area following grafting of Amine 3 to the silica 1 surface, which is in line with expected 'coating' of the porous network of silica 1 by the amine functional agent.

Table 4: Surface area analysis and pore volume of silica1 and grafted silica

Sample	BET surface area (M2g-1)	Pore volume / cm2g-1
silica	194.2	0.45
CSiAmG2	54.7	0.0018

Characterization of nitrogen-rich porous polymer materials

Characterization of Polymer 1 and Polymer 2

The polymers displayed large surface areas as expected and very close to literature reports and therefore it can be concluded that the materials were successfully synthesised. The polymer 1 had double the surface area when compared to the Polymer 2 (Table 5). The cumulative micropore volume that was double (0.23985 cm3/g) that of polymer 1 (0.101445 cm3/g). When the ultra-micropore volumes are analysed, the polymer 1 also has a larger cumulative volume compared to the polymer 2. It is expected that polymer 1 should have higher CO2 capacity because it has larger cumulative volumes in the micropore and ultra-micropore regions. Such materials display high physisorption when they interact with CO2 capture.

Table 5. Surface area and pore volumes of the polymers measured using BET

Sample	Surface area (m2/g)	Total pore volume (cm3/g)	Cumulative micropore Volume (cm3/g)	Cumulative ultra micropore volume (cm3/g)
Polymer 2	392.3	1.53	0.10	0.014
Polymer 1	741.3	1.10	0.24	0.09

Characterisation of Polymer 3 and Polymer 4

To determine the successful grafting of Amine 1 or Amine 2 onto Polymer surface, a thermal decomposition of the Polymer, Polymer 4 and polymer 3 was conducted using thermogravimetric analysis. Figure 9 shows the plots for the experiments.

Figure 9. TGA and DTG for thermal decomposition of Polymer (orange), Polymer 4 (green) and Polymer 3 (blue).

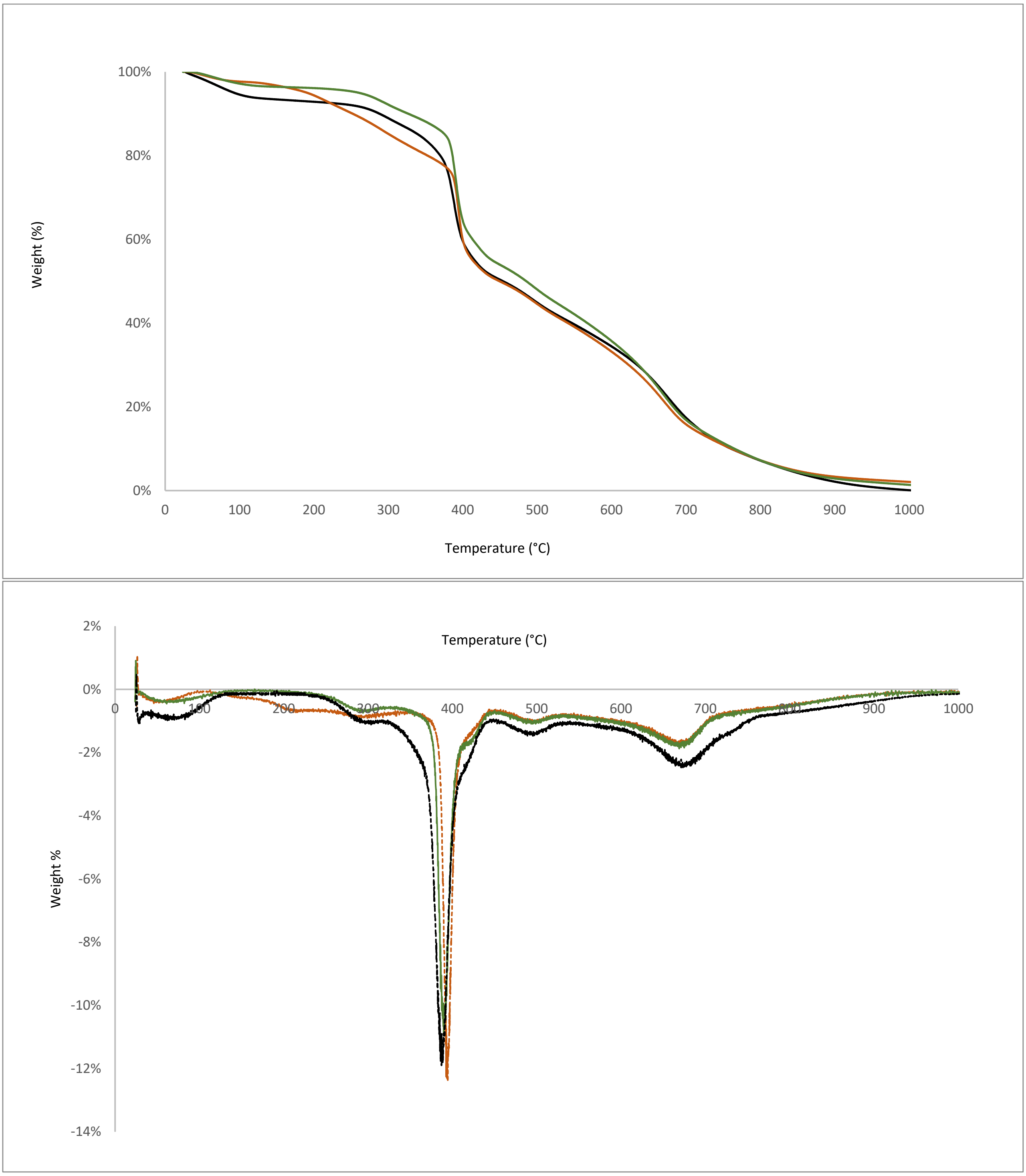

The results show three main weight loss steps below the temperature of 450 °C. The first weight loss is due to decomposition of free nitrogenous based materials and residual moisture. The second step between 130 and 260 °C is due to loss of coordinated nitrogenous based materials which is related to the amount of hydroxide based content in the material. And then at temperature >260 °C, a combination of polymer decomposition and free amine decomposition is observed. In the temperatures highlighted (circled) in Figure 10), differences are observed between grafted polymers and material before amine grafting. The decomposition due to coordinated nitrogenous materials which is related to hydroxide based content is absent in Polymer 3 and polymer 4 indicating the absence of hydroxide based groups.

The polymers were also characterised using FTIR spectroscopy, to identify the functional groups present in the materials (Figure 10).

Figure 10: FT-IR spectra of the polymer substrate, polymer 3 and polymer 4.

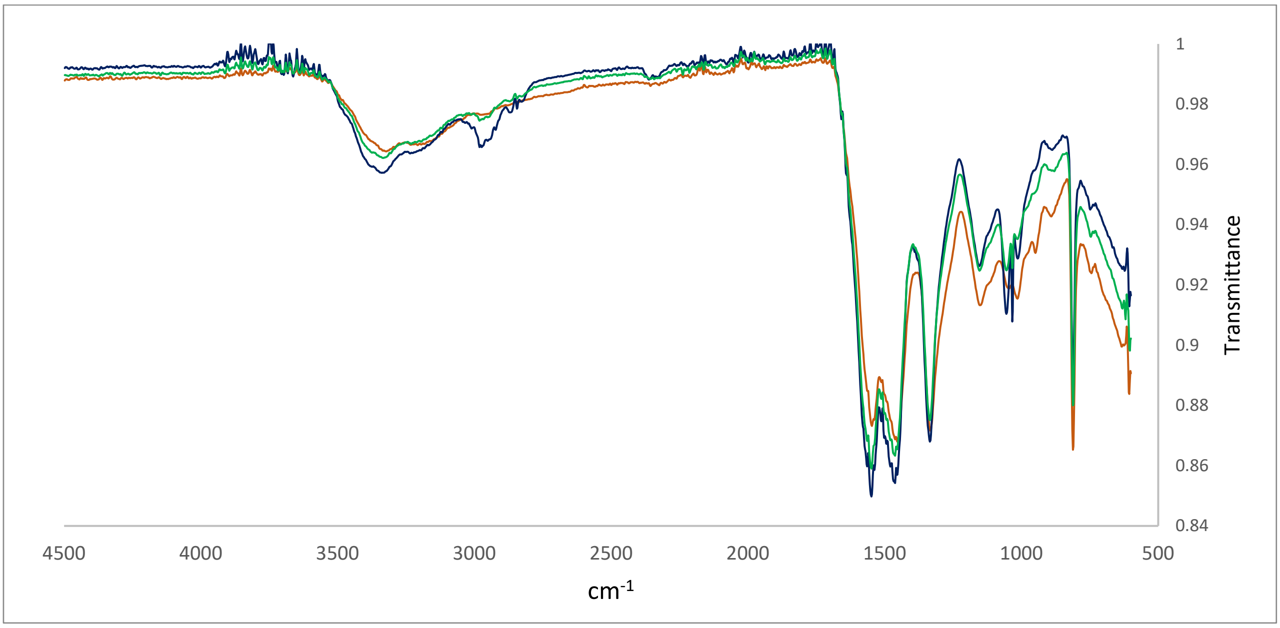

The spectrum shows the characteristic peaks expected for the functional groups present in the polymers.

Work Package 1.4 – Measurement of CO2 loading capacities in various conditions

CO2 sorption experiments were conducted through the use of either isothermal or thermal-step thermogravimetric analysis (TGA). CO2 sorption analysis by TGA (Figure 11) operates through analysing the mass changes of small (~10-20 mg) samples of sorbent materials following the passing of gas mixtures containing CO2. The standard gas mixture used in experiments is 4:1 CO2 to N2 as a minimal flow of N2 is required to protect the thermostated balance operation. From this, minute mass changes (up to 0.1µg) can easily be observed as a function of time in a facile and accurate manner, excluding the effects of atmospheric impurities such as water (which can be removed in-situ through a prior heating step at 110°C for 1 hour prior to CO2 sorption). Typically, CO2 sorption is followed for 60 minutes at the appropriate temperature, due to the fact that with the small sample size this represents a significant quantity of CO2 passed over the sample. CO2 sorption can be easily evaluated through essentially the same experiment, where CO2 is loaded on the sample and the mass loss over a period of time is followed closely.

Figure 11: Diagram of TGA-DSC operated by C4C in evaluating CO2 adsorption/desorption.

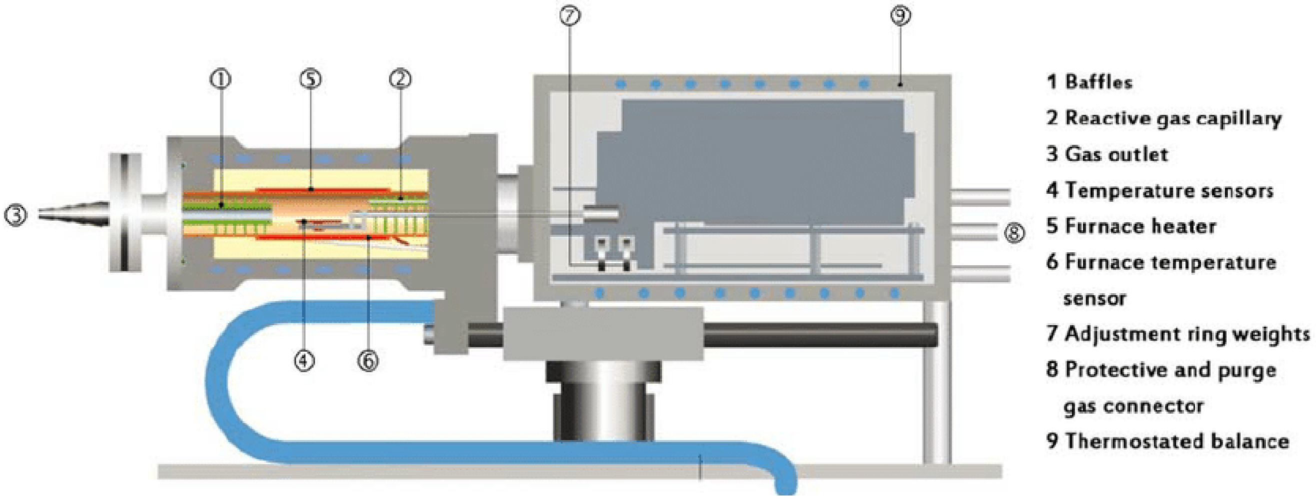

Limitations of TGA CO2 sorption analysis are mostly centred around the fact that gas pressure is limited to 10 bar: thus increased pressure experiments are not possible. As a result, autoclave CO2 loading, performed at any given temperature over 12 hours was conducted at 10 bar, with the mass of samples being evaluated after adsorption to give the quantity of CO2 adsorbed. Table 6 summarises the techniques used to evaluate CO2 sorption.

Table 6: Summary of CO2 sorption studies utilized at this phase in the study

Technique	What is observed	Benefit
TGA (Gravimetric CO2 sorption)	CO2 sorption by change in mass	Highly accurate, dynamic and can measure CO2 adsorption and desorption under high controlled environment. Can only measure under atmospheric pressure
Autoclave (High pressure)	CO2 sorption under increase pressure	Less accurate, can modulate pressure easily.

Measurement of CO2 loading capacity on nitrogen enhanced silicas

Effect of silica substrate CO2 loading capacity on nitrogen enhanced silicas

Porous silicas are chemically and thermally stable materials with uniform pore sizes, distribution, high surface area and high adsorption capacity. The size and shape of porous silica particles as well as the structure of pores can be fine-tuned by controlling synthetic parameters such as temperature, reaction time, amount of silica source or changing calcination temperature. These materials are versatile and depending on their structure different carbon dioxide capture capacities may be observed. Silica 1 and silica 5 impregnated with varying concentrations of Amine 1.1 and their CO2 adsorption capacities evaluated. Silica 1 is less dense than Silica 5 which has a larger surface area. Silica 1 has large pores compared to Silica 5.

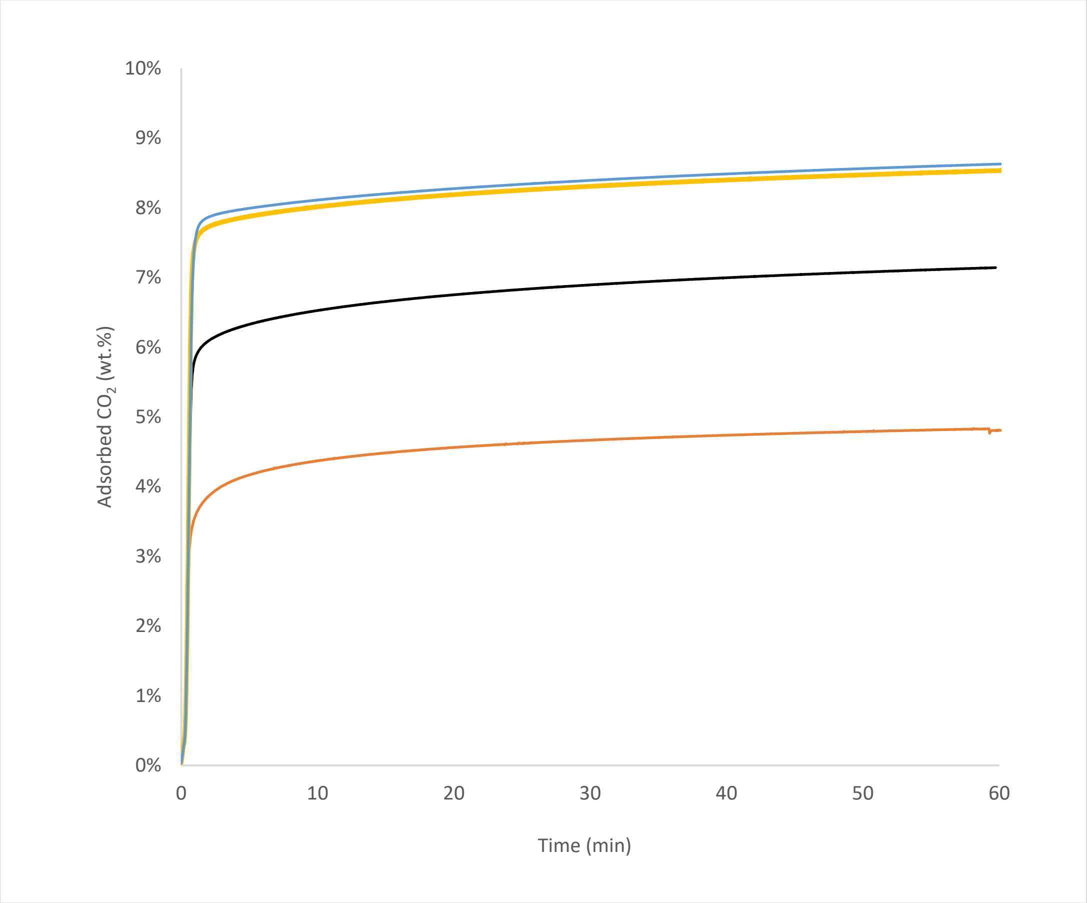

Figure 12. Adsorption profiles of Silica 1 nitrogen enhanced silicas (Conditions: CO2 80%, N2 20% at 100 mL min-1, 25°C measured over 60 minutes). Blue Silica 1 – amine 1.1, Orange Silica 1 Amine 1.2, Blue Silica 1 Amine 1.3 and red Silica 1 Amine 1.4.

Figure 13. Adsorption profiles of Silica 5 impregnated nitrogen enhanced silicas (Conditions: CO2 80%, N2 20% at 100 mL min-1, 25°C measured over 60 minutes). Blue Silica 5 – amine 1.1, Orange Silica 5 Amine 1.2, Blue Silica 5 Amine 1.3 and red Silica 5 Amine 1.4.

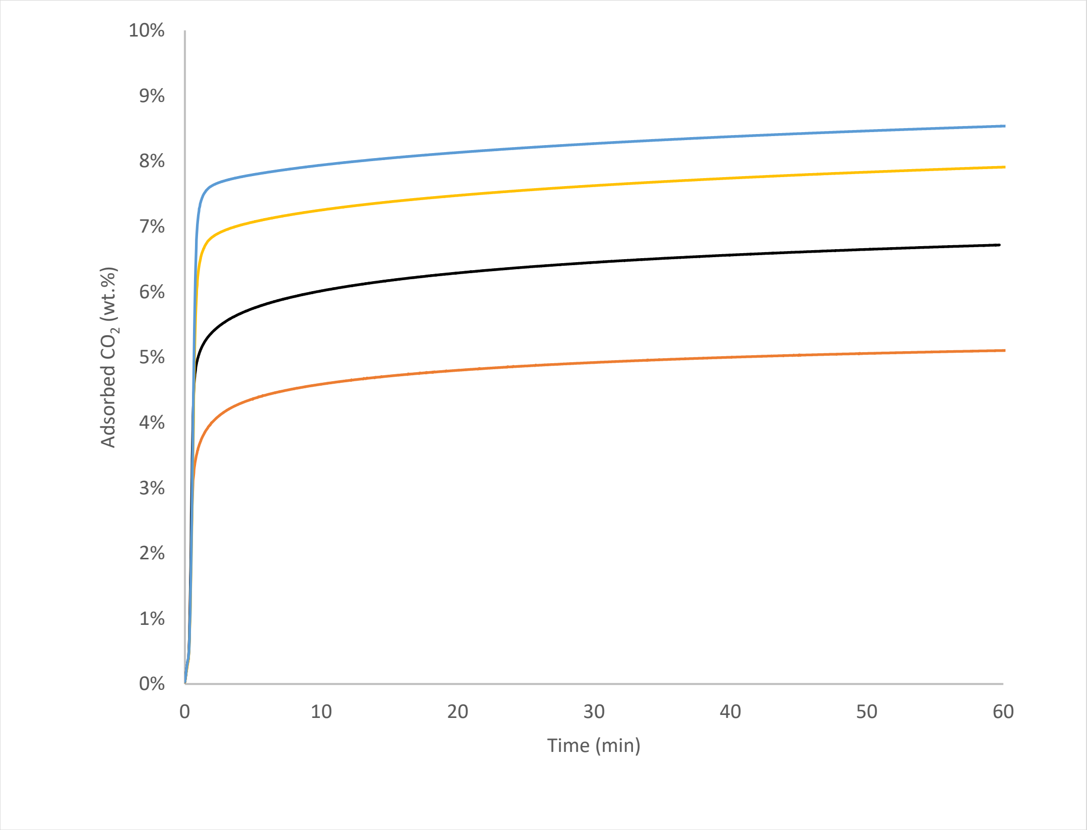

Both silicas were loaded with amine 1 at various concentrations and both displayed comparable capture capacity as shown, this demonstrates that silicas can be effective for carbon capture for concrete.

Effect of amine identity on CO2 loading capacity on amine impregnated silicas

Figure 14. (Adsorption profiles of Silica 2 Amine 2 impregnated silicas (Conditions: CO2 80%, N2 20% at 100 mL min-1, 25°C measured over 60 minutes) black Silica 2 amine 2.1, orange silica 2 with amine 2.2 and blue silica 2 with amine 2.3.

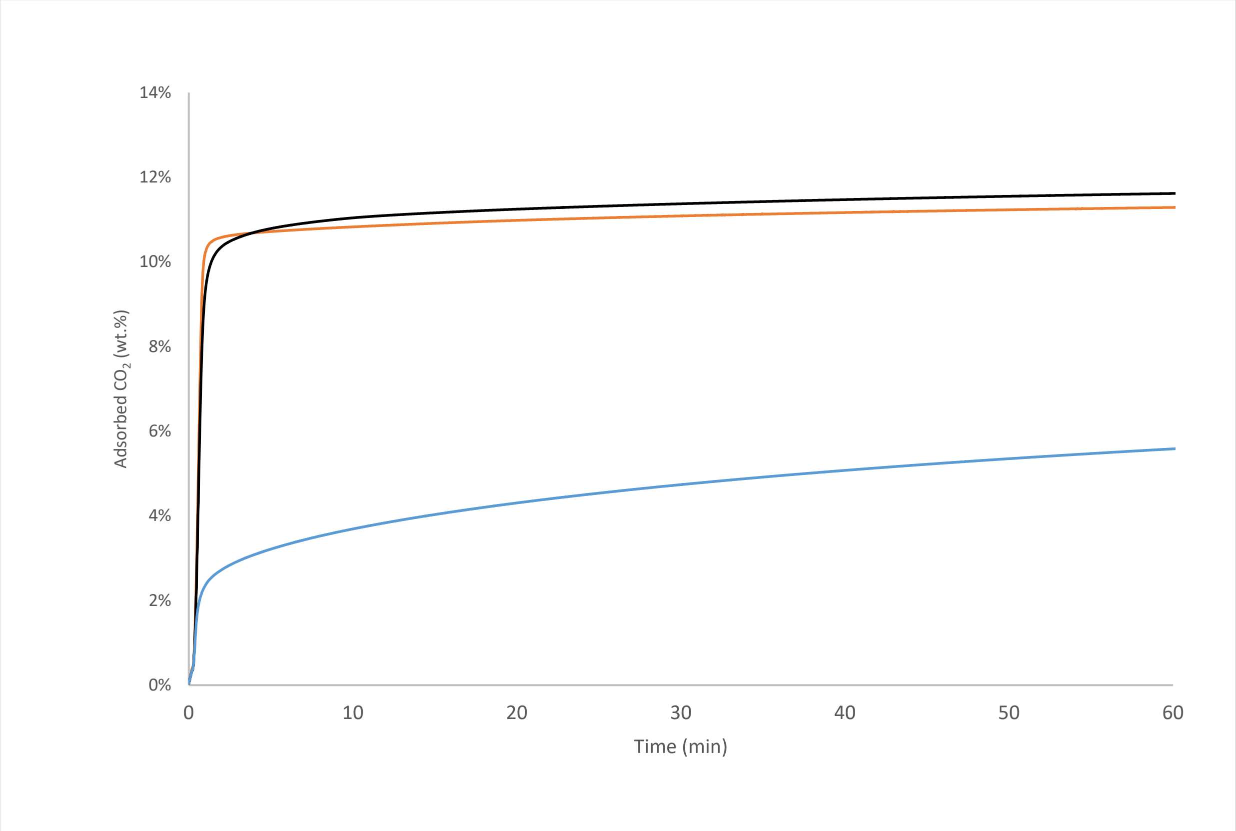

Figure 15. (Adsorption profiles of Silica 1 Amine 2 impregnated silicas (Conditions: CO2 80%, N2 20% at 100 mL min-1, 25°C measured over 60 minutes) orange silica 1 with amine 2.1 and blue silica 1 with amine 2.2.

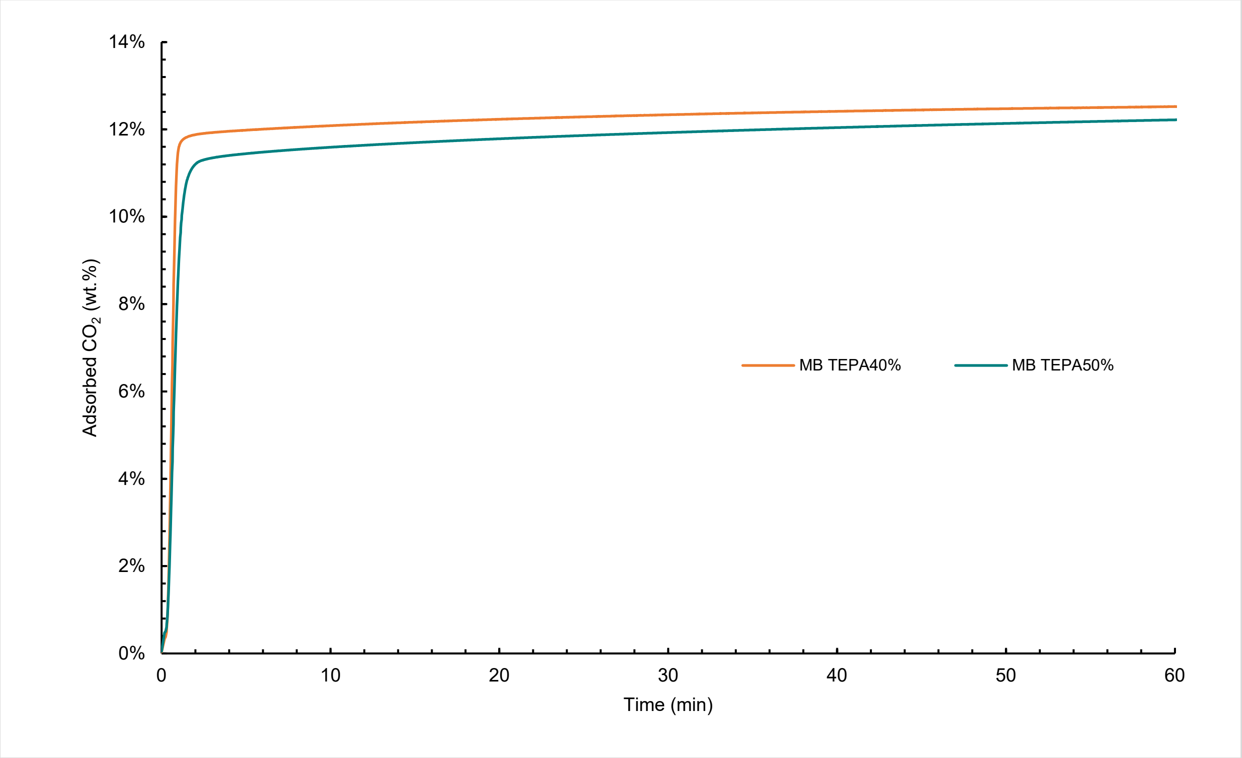

Silica 2 and silica 1 were impregnated with amine 2, and showed the greatly increased CO2 capacities, a significant improvement in comparison with amine 1 silicas .

Measurement of CO2 loading capacity of nitrogenously enhanced silicas

Amine incorporated carrier precursors CSiSG1-3 also demonstrated comparable CO2 sorption results to grafted samples at atmospheric pressure, with maximal CO2 capacities of 6.24 wt%. The sol-gel produced carriers, therefore, represent significantly more accessible amine, likely due to the more homogenous surface-coverage achievable though the particle synthesis.

Table 7 Summary of TGA probed CO2 adsorption of Nitrogenous enhanced silicas

Sample	CO2 capacity / mMol g-1	CO2 capacity / wt%	Amine efficiency / %
CSiSG3	1.42	6.24	43
CSiSG2	1.23	5.43	40
CSiSG1	1.15	5.06	48

Figure 16: CO2 adsorption of nitrogen enhanced silicas. Conditions: CO2 80%, N2 20% at 100 mL min-1, 25°C measured over 60 minutes) Blue – Silica 3 amine 3.1, Silica 3 amine 3.2 and Silica 3 amine 3.3

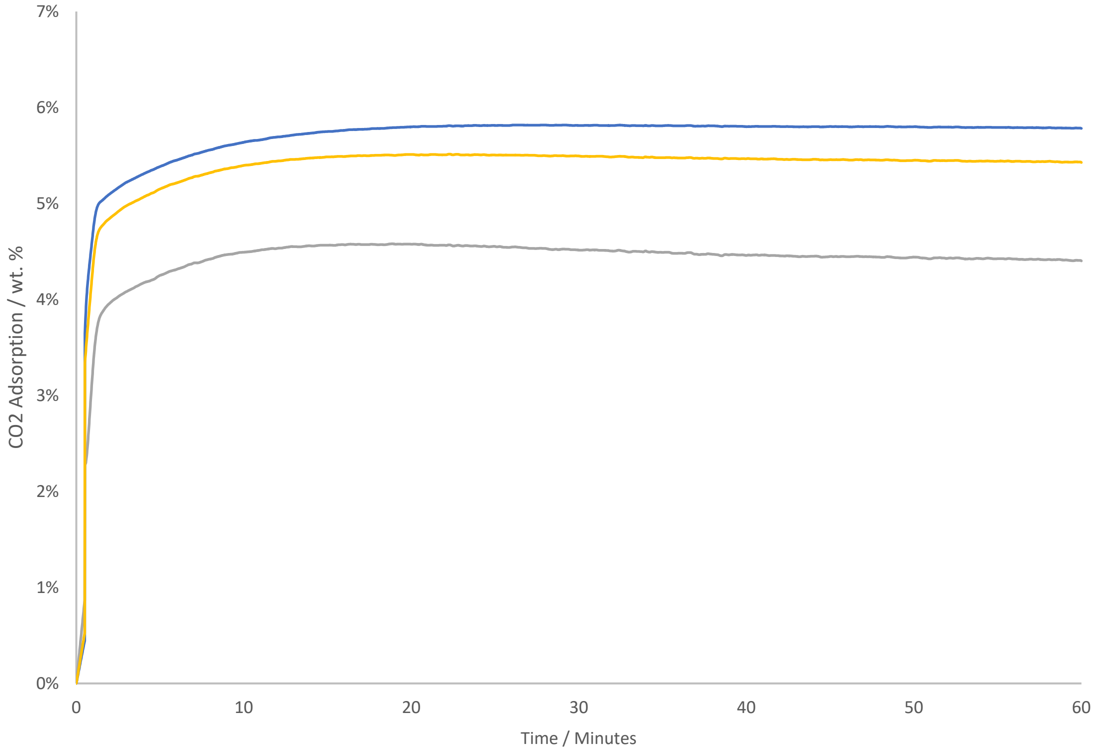

Measurement of CO2 loading capacity on nitrogen enhanced silicas

Experiments detailed the optimal CO2 sorption temperature for amine grafted silicas to be ~75°C, thus all CO2 adsorptions were performed at this temperature. Following adsorption at this temperature, the temperature was reduced to 25°C whereupon some further adsorption took place. This is interpreted as an initial chemisorption (which we are targeting) followed by non-specific physisorption. In all cases the physisorption component was comparatively minor, suggesting that these carriers adsorb CO2.

CO2 capacities of the grafted silica samples CSiAmG1-4 (Table 8, Figure 16) demonstrate somewhat moderate CO2 capacities of up to 6.2 wt%. In comparison to the highest-adsorbing amine-impregnated silicas these values lower, suggesting a reduction in chemisorption activity in comparison with grafted silicas. This is, however, to be expected: these current carrier candidates are monoamines grafted to the silica surface, in comparison with polyamine used in grafting. As such- the amine density on the surface is significantly lower. Assuming the formation of ammonium carbamate species during the chemisorption reaction, one would expect a maximal efficiency of 50% (2 amines to 1 CO2). It can clearly be seen that here; we are approaching this maximal efficiency in comparison to Amine 1.1 silica 1 with a maximum of ~20% (with rough assumptions of 22 amine units per amine 1). This is likely due to the increased surface area of the nitrogen enhanced carriers with respect to the nitrogen enhanced carriers; where a significant quantity of the amine is not exposed to the particle surface and thus their reaction with CO2 is limited by diffusion of CO2 through amine 1. This can be supported by the shallower adsorption profile of CSiAmG1 in Figure 17.

Figure 17: CO2 adsorption traces of grafted silicas CSiAmG4 (blue solid line), CSiAMG3 (red solid line), CSiAmG2 (green solid line). CSiAmG1 (yellow solid line) at 75°C (until 60 minutes) then at 25°C. (Conditions: CO2 80%, N2 20% at 100 mL min-1, 75°C measured over first 60 minutes, then 25% for 40 minutes)

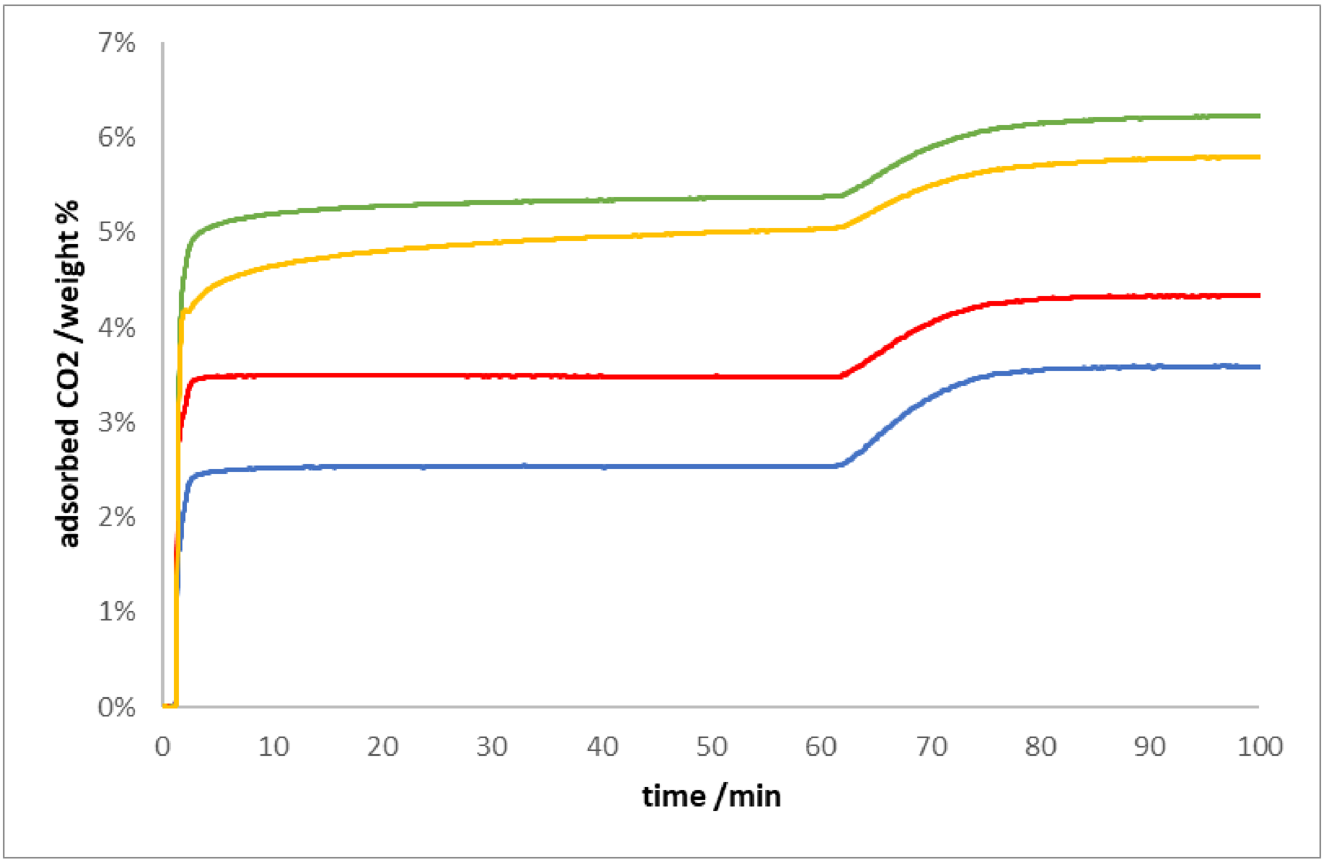

Table 8. Autoclave CO2 experiments with static 10bar of 100% CO2 immediately and after air exposure

Sample	CO2 capacity / mMol g-1	CO2 capacity / wt%	Amine efficiency / %
CSiAmG2	1.42	6.24	26
CSiAmG3	1.32	5.821	18
CSiAmG1	1.00	4.231	40
CSiAmG4	0.661	2.891	30

Autoclave adsorption experiments were performed at a CO2 pressure of 10 bar, at 75°C overnight (Table 9). Again, CSiAMG2 exhibited maximal CO2 capacity, roughly 2% higher than that observed at atmospheric pressure. Interestingly, CSiAmG3 exhibited the highest CO2 loading when loaded at 10bar, in contrast to atmospheric pressure experiments. This is in line with observations on the pore-volume and surface areas, where one would expect the higher loading to 'block' the pores requiring a significant diffusion barrier to be overcome by increasing the system pressure. In summary, the most optimal grafted carriers exhibited CO2 capacities more than 9 wt% in their first iterations

Table 9. Autoclave CO2 experiments with static 10bar of 100% CO2 immediately and after air exposure

Time of air-exposure	CSiAmG1	CSiAmG2	CSiAmG3	CSiAmG4
0	2.9%	8.1%	9.1%	5.1%
1	1.5%	7.3%	7.0%	3.8%
3	0.7%	6.5%	6.9%	1.9%
24	1.5%	7.7%	7.8%	3.2%

Measurement of CO2 loading capacity on nitrogen-rich porous polymer materials

CO2 loading capacity of Polymer 1 and Polymer 2

The synthesised polymers, together with one commercially available melamine sponge were tested in CO2 adsorption experiments at 25 °C, 1 bar CO2 for 60 min (14 kj mol-1) (Figure 18). The polymer with the largest CO2 capture capacity is the polymer 2 (8.08 wt%) while the polymer 1 has a CO2 capture capacity of 6.62 wt%. Based on the BET results, it is expected that polymer 1 has higher CO2 capture capacity due to its large surface area of 741.3 m2/g. This polymer also has a larger cumulative ultra micropore volume which favours physisorption. However, contrary to these expectations, the polymer 2 displays better capture capacity for CO2 which could due to firstly, the flexible nitrogen based linker that may allow the material to accommodate gaseous molecules and secondly, the presence of NH functional groups that have a strong affinity for CO2.

Figure 18. CO2 adsorption profiles of Polymer 1 (orange) and Polymer 2 (green) carriers(Conditions: CO2 80%, N2 20% at 100 mL min-1, 25°C measured over 60 minutes)

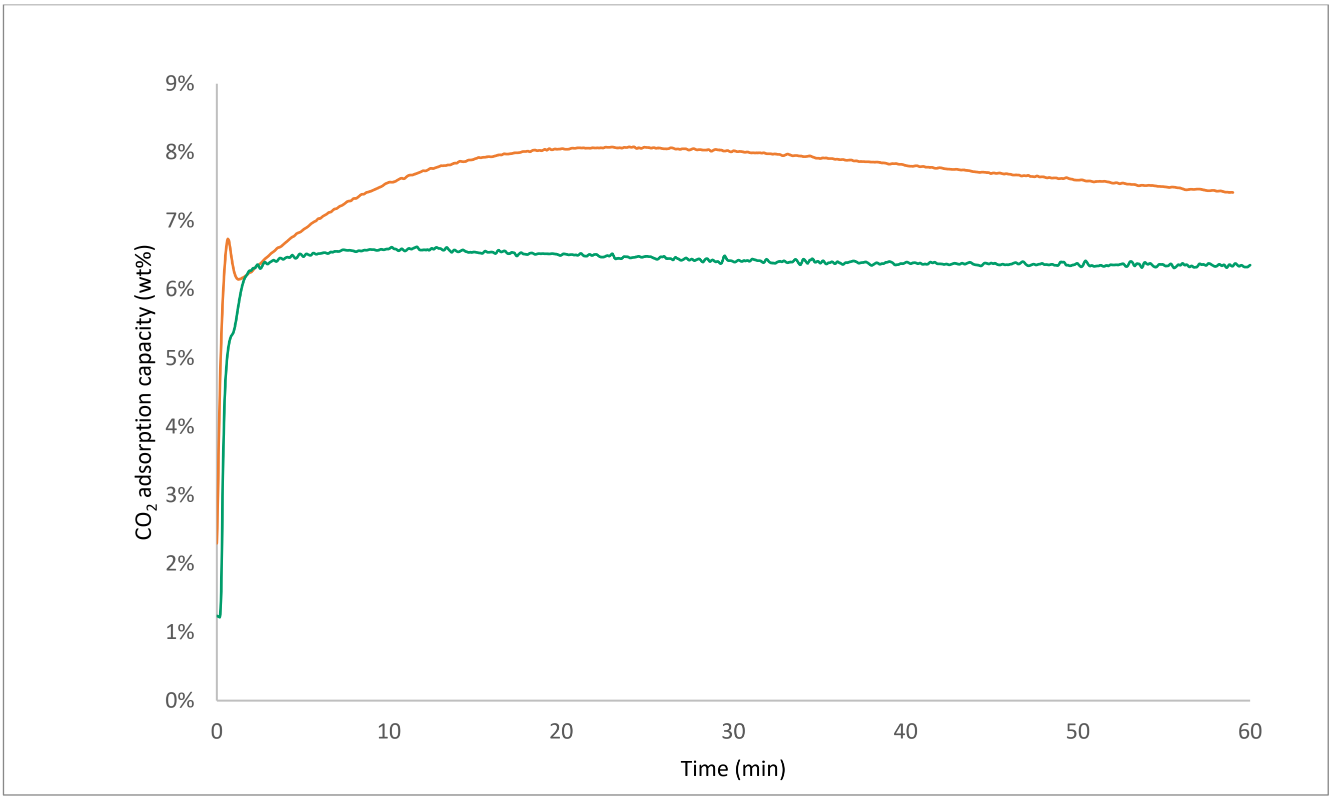

CO2 loading capacity of Amine 2 and amine 1 grafted polymers

The capture capacity of both polymers at 25 °C was found to be 2.71 wt% and 3.00 wt% for Polymer 1 amine 2 and polymer 2 amine 1 respectively (Figure 19). The polymer with amine 1 grafted has better capture capacity while the rate of release of CO2 is slower for amine 2 grafted polymer.

Figure 19: CO2 adsorption traces of Polymer 1 – amine 1 (green) and polymer 1 – amine 2 (orange) at either 75°C or 90 °C, CO2 80%, N2 20% at 100 mL min-1 (for 60 minutes) then at 25°C for 60 min.

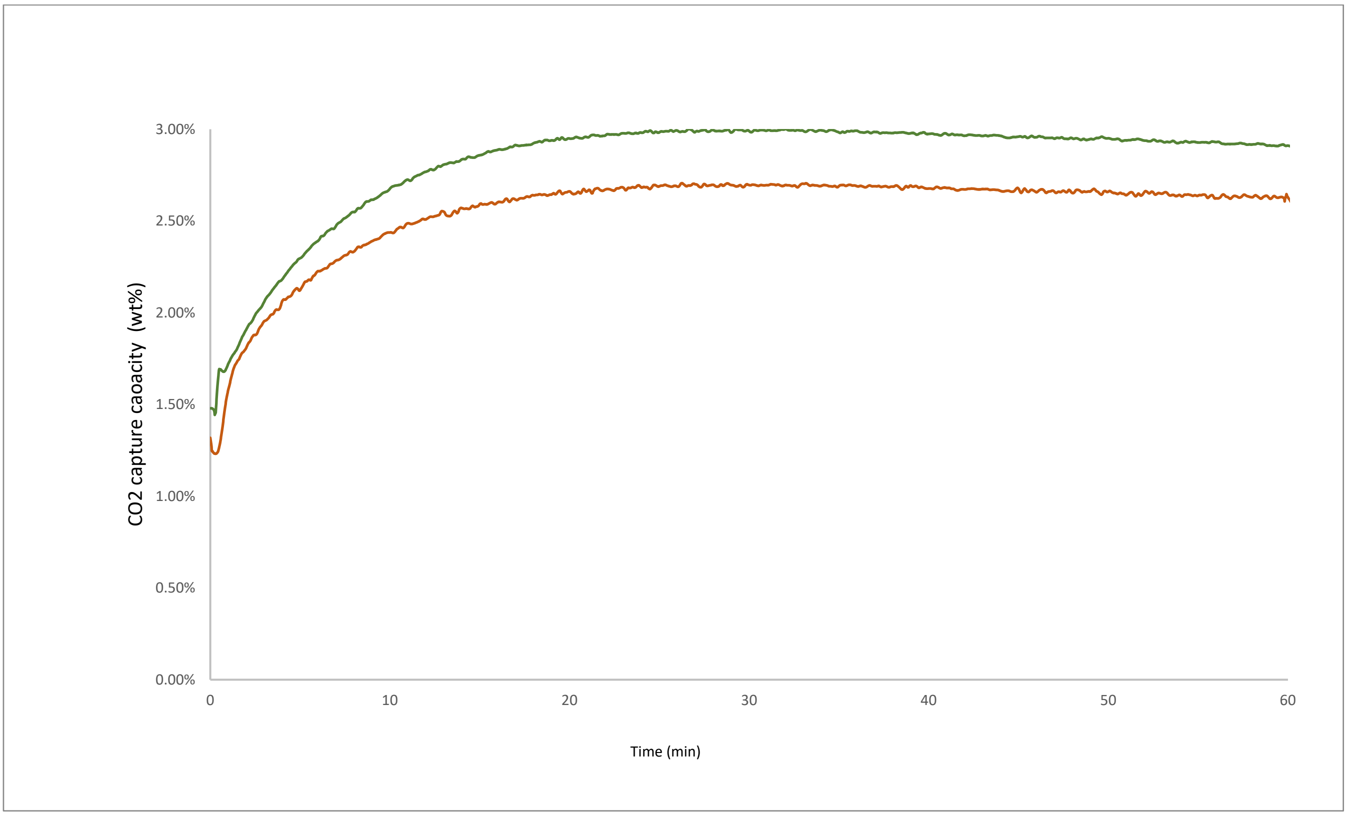

Table 10. CO2 adsorbed during TGA CO2 adsorption at 75°C - 25 °C and 90 °C – 25 °C, 1 bar CO2, 100ml/min.

Sample	Temperature (°C)	CO2 capacity
Polymer 1 – amine 2	75 -25	0.63 wt% (75 °C) 1.29 wt% (25 °C) Total = 1.92 wt%
	90 - 25	0.65 wt% (90 °C) 2.19 wt% (25 °C) Total = 2.84 wt%
polymer 1 – amine 1	75 - 25	0.59 wt% (75 °C) 1.43 wt% (25 °C) Total = 2.02 wt%

Sample	Temperature (°C)	CO2 capacity
	90 - 25	0.79 wt% (90 °C) 2.53 wt% (25 °C) Total = 3.32 wt%

Both polymers show very strong chemisorption interactions with CO2 under the tested conditions on TGA at 75 ° and 90 °C under 1 bar CO2 atmosphere.

Measurement of CO2 loading capacity on amine 3 inspired materials

CO2 capture capacity of the amine 3 inspired materials

The CO2 absorption capacity of amine 3 was investigated using two different methods. In the first method, carbon dioxide was bubbled into a known amount of amine 3 (Figure 11), and the weight was determined by weighing the reaction mixture every 30 minutes until a constant weight was obtained. After 90 minutes, a constant weight of 0.157 g giving a CO2 capture capacity of 1.47 wt%.

Figure 20. CO2 bubbling into amine 3 inspired material.

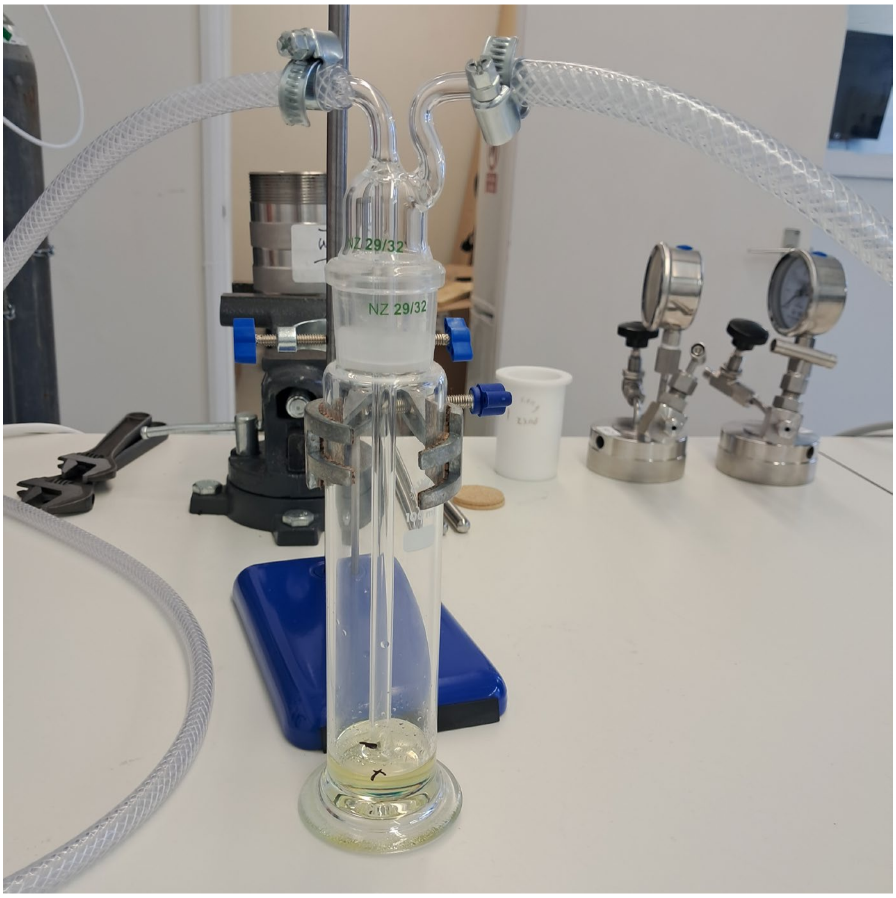

Like amine 3, the amine 3 inspired material's CO2 capture capacity was investigated using two different methods. In the first instance CO2 was bubbled into the liquid at room temperature and in the second test, the experiment was performed on the TGA at 25 °C for 1 hour. In the bubbling experiment, the weight increase was 1.352 g which translates to 12.43 wt% CO2 loading.

The results for the CO2 adsorption experiments conducted at 25 °C under 1 bar CO2 (TGA) are summarised in table 20. All the materials show CO2 capture capacity that is below 5 wt%.. However, it is also important to note that, the materials did not reach their full capture capacity in 1 h TGA experiments as seen in the graphs in Figure 19. After analysis using BET, an erroneous result was obtained due to the material having very little area, and this could also have attributed to the poor capture capacity. The carrier with the highest CO2 capture capacity is polymer 1-amine 3-liqu (3.94 wt%) and the lowest capacity was reported for polymer 1-amine 3-amine 1 (2.91 wt%) as summarised in Table 15.

Table 11. Summary of CO2 adsorbed at 25 °C, CO2 80%, N2 20% at 100 mL min-1, 60 minutes then at 25°C,1 h (TGA) and 75 °C, 16 h (autoclave), 10 bar CO2 pressure.

Sample	CO2 capacity (TGA – 25°C ,1h)	CO2 Capacity (Autoclave – 75 °C , 16h)
Polymer 1 amine 3 (Dark blue)	3.74 wt%	4.72 wt%
Polymer 1 amine 3-liq	3.94 wt%	9.33 wt%
Polymer 1 amine 3-amine 1 (13 wt%)	3.51 wt%	10.67 wt%
Polymer 1 amine 3 - amine 1 (19 wt%)	2.91 wt%	11.67 wt%

The amine 3 polymer 1 displays CO2 capture capacity of 3.74 wt% at 25 °C and retains only 7 wt% after 1 hour desorption experiment under nitrogen using thermogravimetric analysis (Figure 21). The absence of amine results in fast desorption because the material does not form a mixed carbamate that is stable which ultimately affects the release rates. It was also clear that the materials containing amine 2 had slow rates of CO2 release, even though the capacity was low (<5 wt%).

Figure 21. 1 bar CO2 at 25 °C, CO2 80%, N2 20% at 100 mL min-1 (for 60 minutes). Polymer 1 – amine 3 – liq (orange), Polymer 1 – amine 3 (dark blue), polymer 1 amine 3 19% Amine 2 (light blue), polymer 1 amine 3 13% Amine 2 (green), Amine 3-liq (olive green)

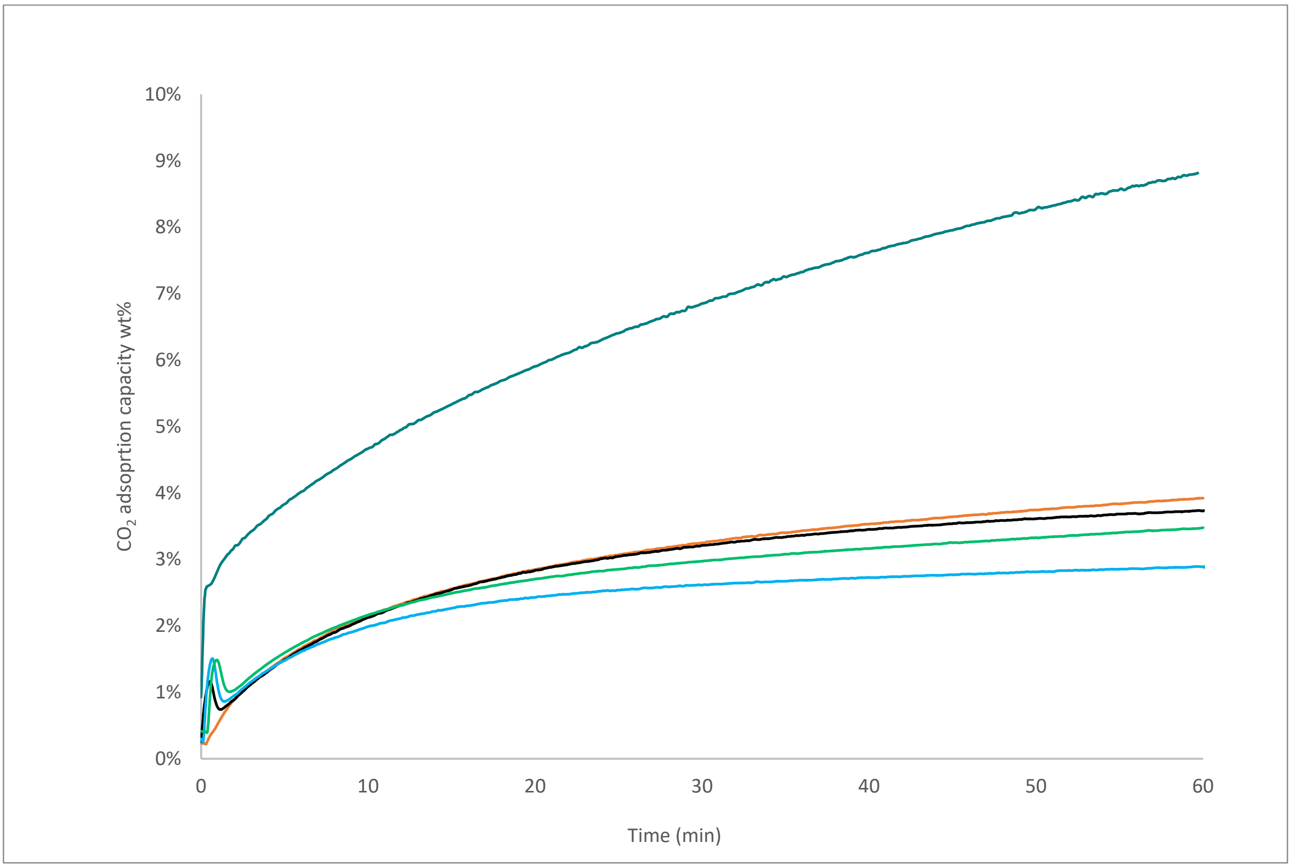

Work Package 1.5 – Measurement of CO2 release rates in various conditions

BET is a measurement of N2 gas sorption for surface area/pore size distribution and gives no information on release rate. TGA is an extremely informative method of accurately measuring CO2 release rates and was used extensively to provide accurate and reliable results.

Measurement of CO2 release rates on nitrogen enhanced silicas

Effect of amine loading on CO2 release rate

After adsorption of CO2 experiments on the TGA, desorption rates were also analysed. It was observed that’s the desorption rates over the timescale were gradual following and initial faster desorption rate within the first 20 minutes (Figure 22).

Figure 22. CO2 desorption as measured by TGA following adsorption for 1 hour: conditions- 1 bar N2 at 80 mL min-1, 25 °C (for 60 minutes). Silica 1 Amine 1.1 (orange), silica 1 amine 1.2 (green), silica 1 amine 1.3 (blue), silica 1 amine 1.4 (grey)

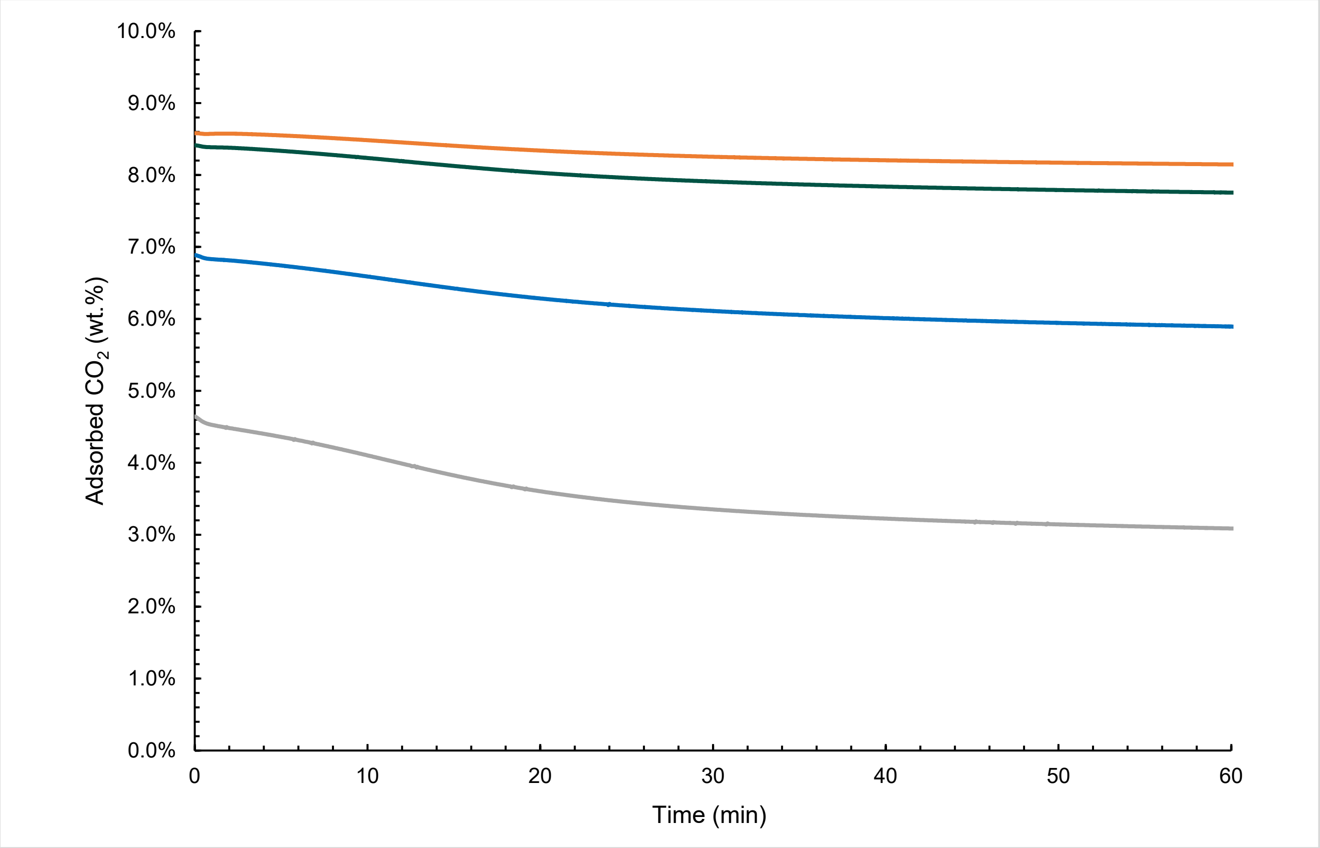

s

These carriers were modified by impregnating Amine 1 of various loadings (1.4, 1.3, 1.2 and 1.1). This resulted in a gradual desorption of carbon dioxide by the carriers at 25 °C. A concomitant increase in CO2 retention was observed alongside amine 1 loading: highlighting the critical effect of amine density/presence on CO2 sorption.

Effect of silica support on CO2 release rate

silica 1 and silica 2 were loaded with amine 1. Both silicas display slow carbon dioxide desorption rates and the various loadings tested (Figure 23). The silicas have similar behaviour, with the amine 1.4 samples showing the fastest release rates in the first 20 minutes which slows down after that as shown in Figure 24.

Figure 23. CO2 desorption silica 1 enhanced with amine 1 at different loadings following 60 minutes at 1bar CO2- conditions: 1 bar N2 at 80 mL min-1, 25 °C (for 60 minutes). (silica 1 amine 1.4 (dashed green), silica 1 amine 1.3 (dashed blue), silica 1 amine 1.1 (purple, silica 1 amine 1.2 (dashed red)

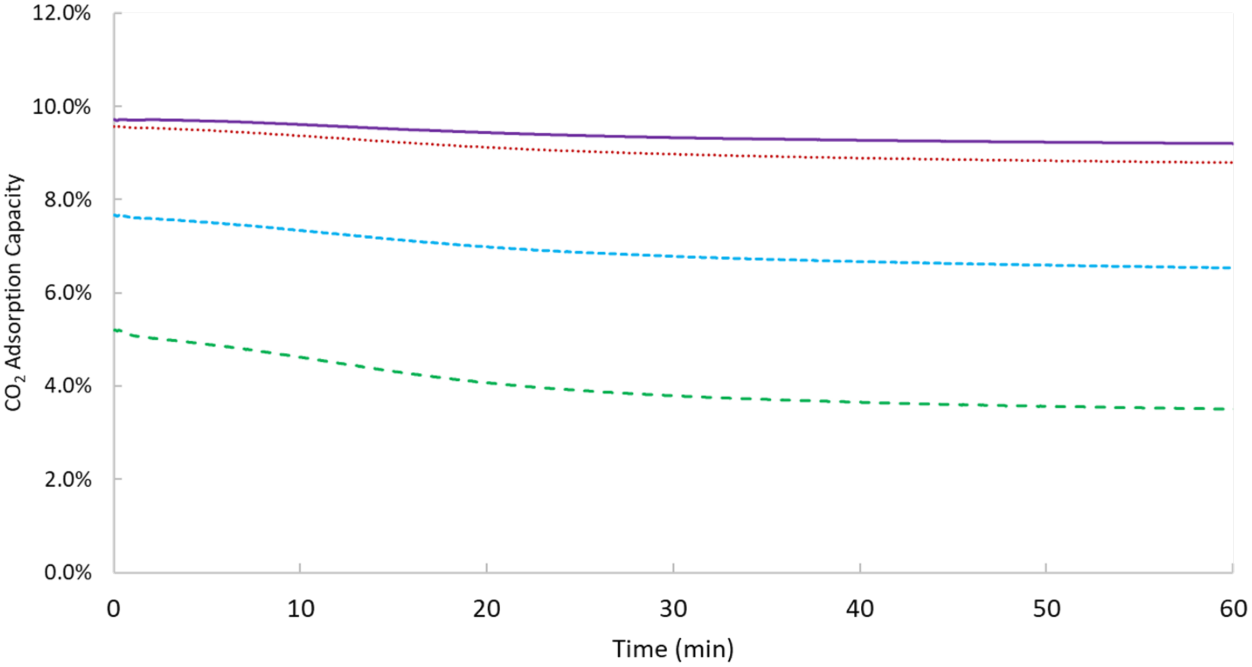

These results show that these silica materials have similar chemical properties even though they have different physical properties such as surface area and density.

Figure 24. CO2 desorption of silica 5enhanced with amine 1 at different loadings following 60 minutes at 1bar CO2- conditions: 1 bar N2 at 80 mL min-1, 25 °C (for 60 minutes). Silica 5 amine 1.1 (purple), silica 5 amine 1.2 (dashed red) silica 5 amine 1.3 (dashed green) and silica 5 amine 1.4 (dashed green).

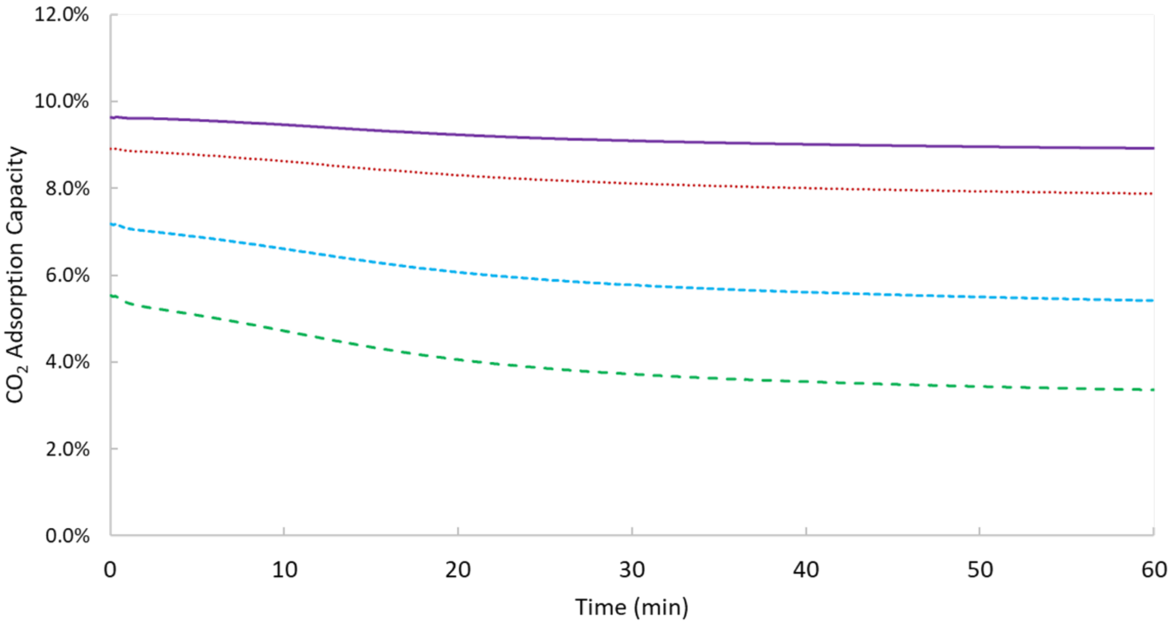

Effect of amine type on CO2 release rate

The type of amine was changed from amine 1 to amine 2 and impregnated into both silica 1 and silica 5.

Figure 25. CO2 desorption of silica 5 impregnated with amine 2 at different loadings following 60 minutes at 1bar CO2- conditions: 1 bar N2 at 80 mL min-1, 25 °C (for 60 minutes). Silica 5 amine 2.1 (dashed blue), silica 5 amine 2.2 (purple) and silica 5 amine 2.3 (dashed red).

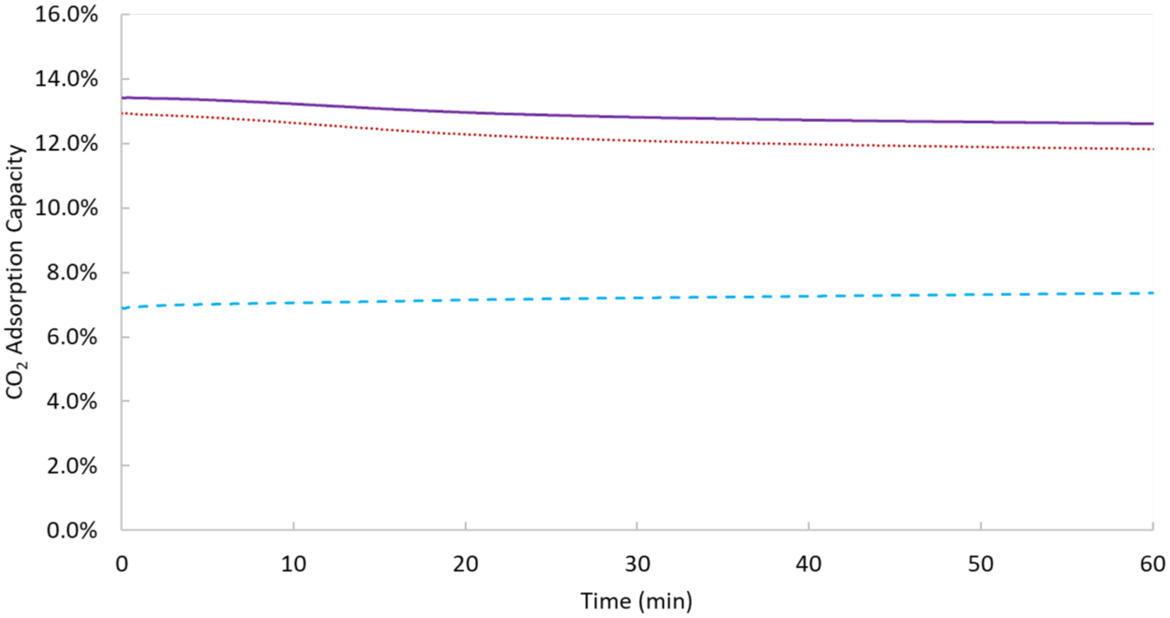

A similar study was conducted using silica 1 amine 2.3 and 2.2 (Figure 26). In both cases, the release rates for carbon dioxide were significantly slower in comparison with amine 1 enhancement. For all the carriers tested, this could be attributed to strong chemisorption interactions which result in slow rates of CO2 release under these conditions. It is not clear at this time the reason the smaller amine 2 is more efficient at capturing, and exhibits slower desorption than amine 1 when impregnated into mesoporous silicas.

Figure 26. silica 1 amine 2.2 (dashed red) and 2.3 (purple) CO2 desorption at different loadings following 60 minutes at 1bar CO2- conditions: 1 bar N2 at 80 mL min-1, 25 °C (for 60 minutes).

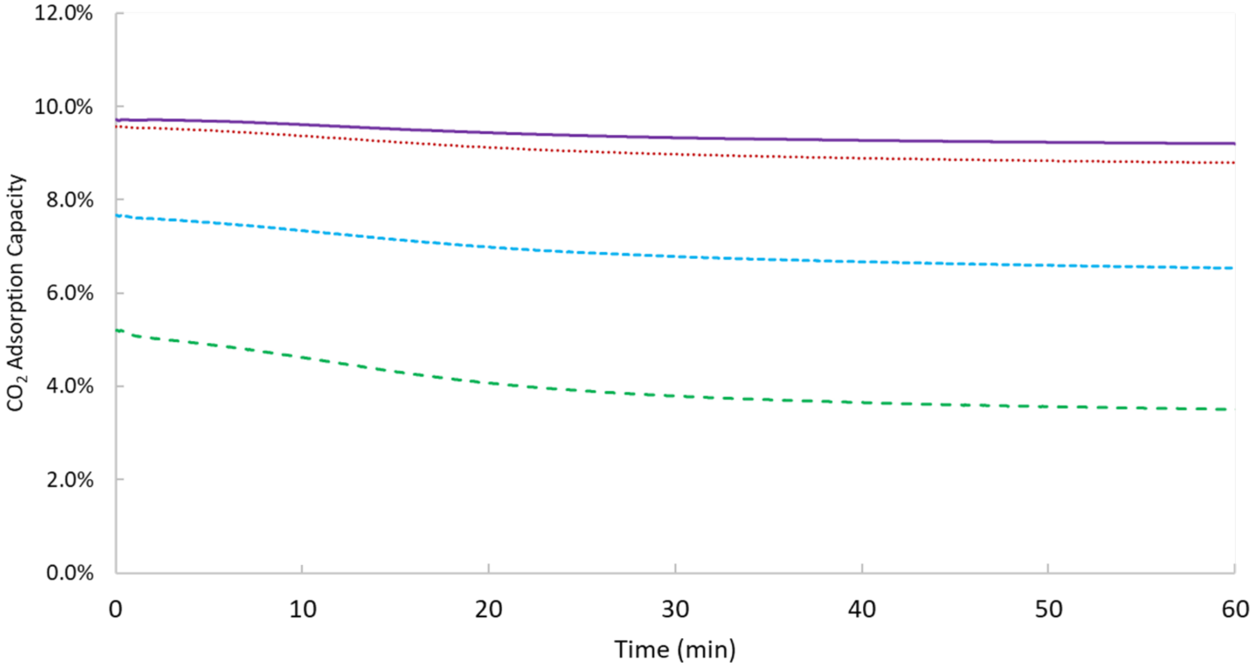

Measurement of CO2 release rates on amine impregnated silicas on amine grafted silicas

Desorption kinetics of the amine-grafted silicas CSiAmG1 (Table 21), trended according to amine 2 loading, with CSiAMG3 demonstrating the slowest apparent desorption followed over 1 hour (with respect to initial loading). Half-lives were calculated according to an exponential fit (R2<0.99) of the desorption traces (Figure 27). Thus, despite not exhibiting the maximal capacity, CSiAmG3 exhibits the slowest desorption kinetics. Desorption kinetics were not reported by Bai et al., and as novel results these CO2 release rates suggest some degree of suitability when considering in-air release rates as carrier materials, with half-lives in the order of several hours (CSiAMG2 and CSiAMG3). It remains to be seen, however, whether the tethering of the amine-functionality in a covalent manner to the porous substrate was enough to ameliorate CO2 desorption kinetics in a cement context. This result suggests a complex interplay with amine-surface density, sample surface area and CO2 capacity and desorption kinetics. Nevertheless, these desorption kinetics of CSiAMG2 and CSiAMG3, whilst faster than in impregnated systems are suitable for the application in cement.

Table 12: Desorption kinetics according to exponential fits of data in Figure 27

Sample	CO2 desorption t1/2 / h
CSiAmG2	148.3
CSiAmG3	503.6
CSiAmG1	3.5
CSiAmG4	0.3

Figure 27. CO2 desorption of CSiAMG1 (purple solid line), CSiAMG2 (red solid line), CSiAmG3 (blue solid line), CSiAmG4 (purple dotted line) following 60 minutes at 1bar CO adsorption2. Conditions: 1 bar N2 at 80 mL min-1, 25 °C (for 60 minutes).

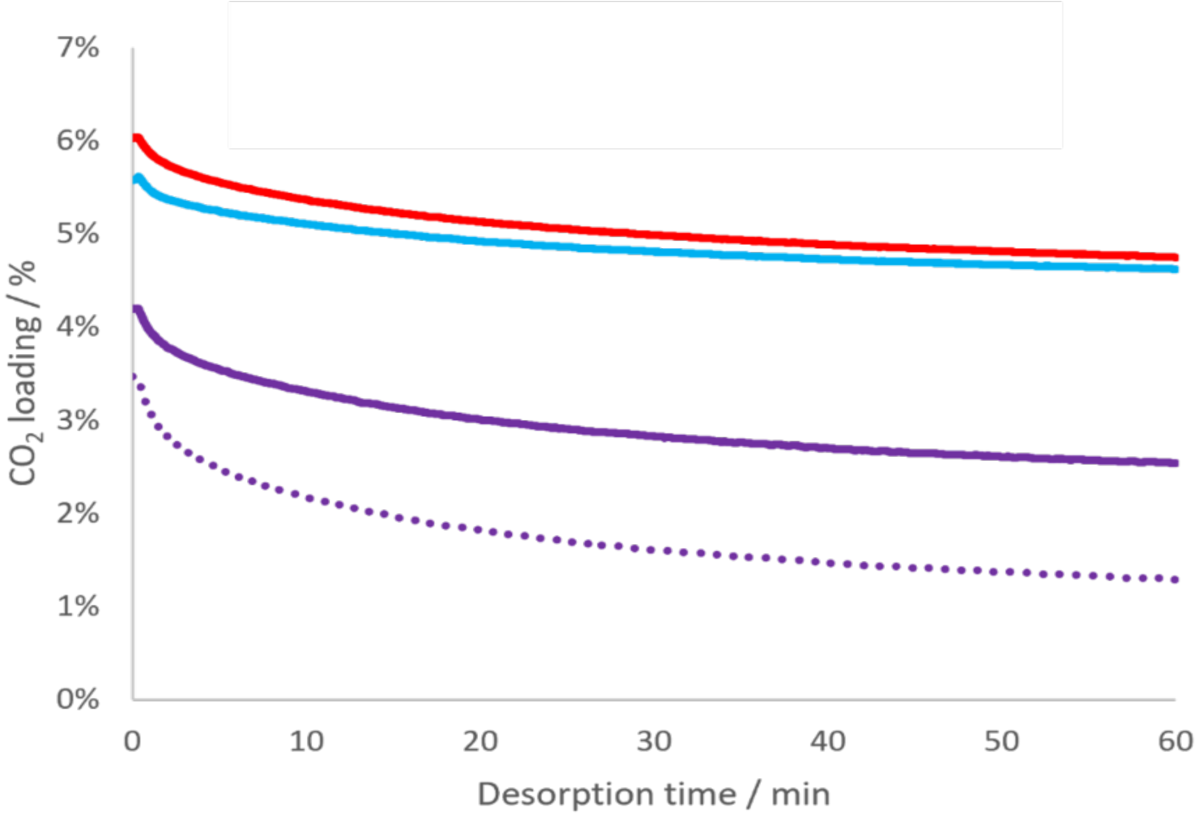

Measurement of CO2 release rates on amine incorporated silicas

CO2 desorption traces of ‘ground-up’ sol-gel amine containing silicas (Figure 28) demonstrated a surprising rapid release of CO2. It is not exactly clear as to why there is such a significant difference in comparison with the amine 2 grafted silica sample in section 8.2, as all sol-gel produced samples released over 50% over the first hour. This could be explained by the more accessible amine species, which resulted in the higher efficiencies observed in the adsorption experiments, as the N2 gas replacement molecules can more efficiently complete for binding sites. It appears therefore, that without further modification these sol-gel amine silicas are not wholly suitable for direct employment in cement relevant conditions.

Figure 28. CO2 desorption of CSiG1 (blue solid line), CSiG2 (orange solid line), CSiG3 (grey solid line), following 60 minutes at 1bar CO adsorption2. Conditions: 1 bar N2 at 80 mL min-1, 25 °C (for 60 minutes).

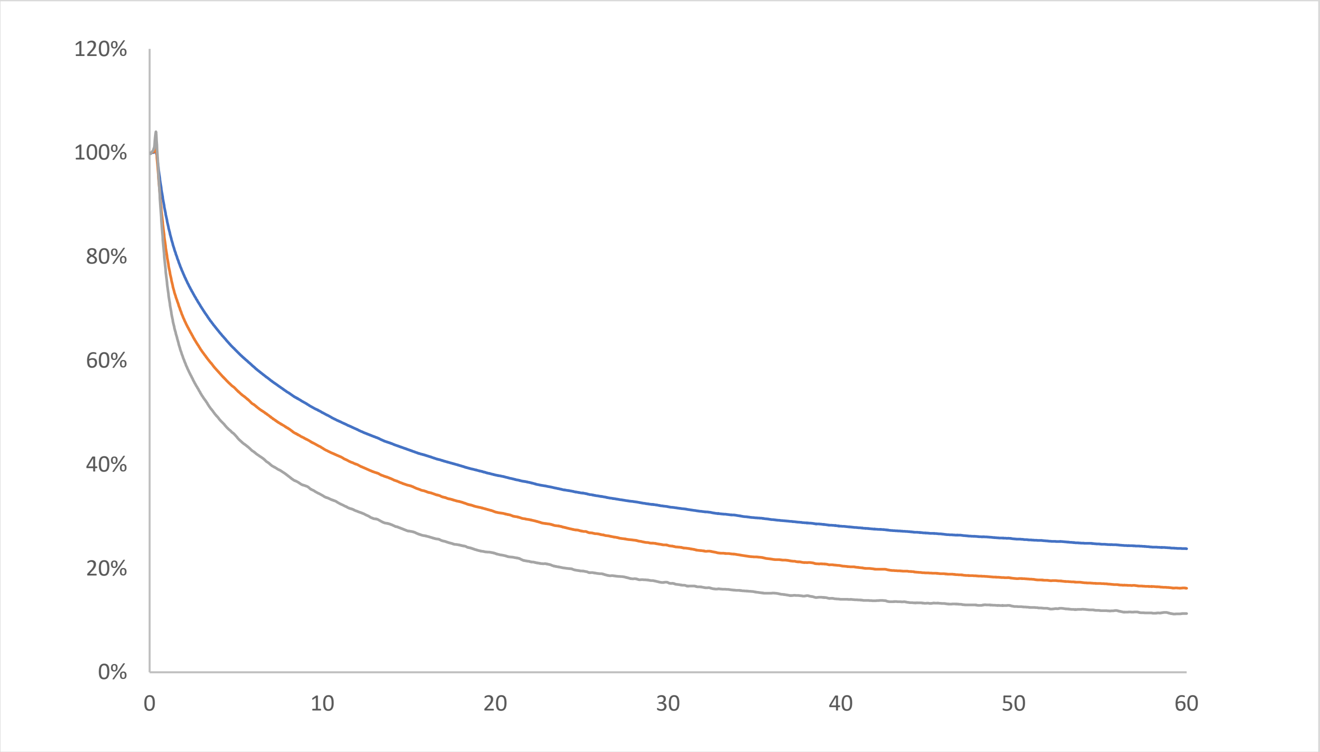

s

Measurement of CO2 release rates on nitrogen-rich porous polymer materials

The nitrogen enhanced polymers were also tested in CO2 desorption experiments. These were conducted at 1 bar N2 pressure, at 25 °C for 1 h. The results obtained for these studies are summarised in Figure 29 below.

Figure 29.CO2 desorption of polymer 1 (brown) and polymer 2 (olive green) following 1 hour of CO2 adsorption at 1 bar. 1 bar N2, at 80 mL min-1, 25 °C (for 60 minutes).

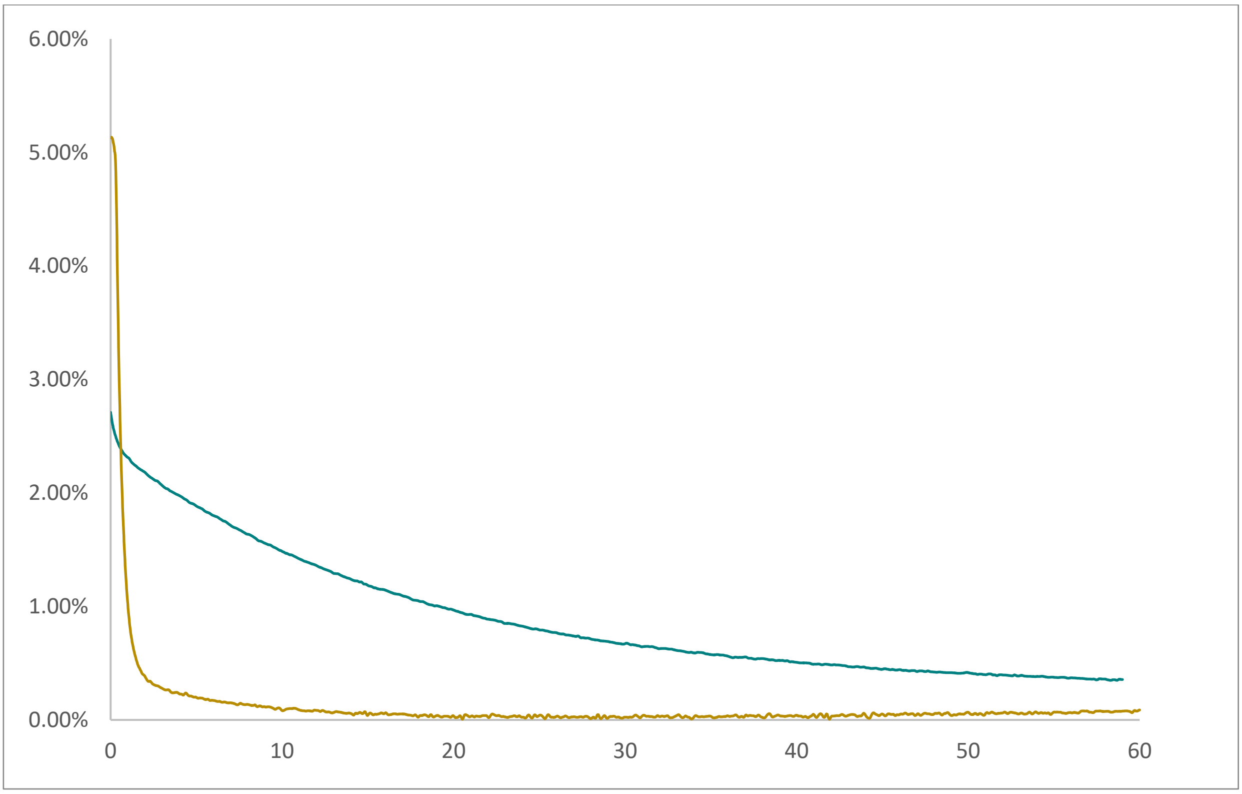

The polymer 1 release 100% of the captured CO2 within the first 10 minutes of the desorption experiment. The polymer 2 also shows slower desorption rates when compared to the polymer 1 counterpart and this slightly slower desorption could be due the presence of NH- groups present in the polymer. However, it is thus apparent that these are not able to undergo CO2 chemisorption to form species such as carbamates.

The polymers enhanced with amine 1 and amine 2 were also tested in the desorption experiments at 25 °C, 80 mL/min N2 flow rate for 60 minutes (Figure 30). The results are summarised below. The temperatures indicated in the legend show the CO2 adsorption experiment temperatures.

Figure 30: CO2 desorption of polymer 1 grafted with amines 1 and 2 following 1 hour of CO2 adsorption at 1 bar. Conditions: 1 bar N2 at 80 mL min-1, 25 °C (for 60 minutes). Polymer 1 amine 1 25°C (green), Polymer 1 amine 2 25°C (yellow), Polymer 1 amine 1 75°C (blue), Polymer 1 amine 2 75°C (brown).

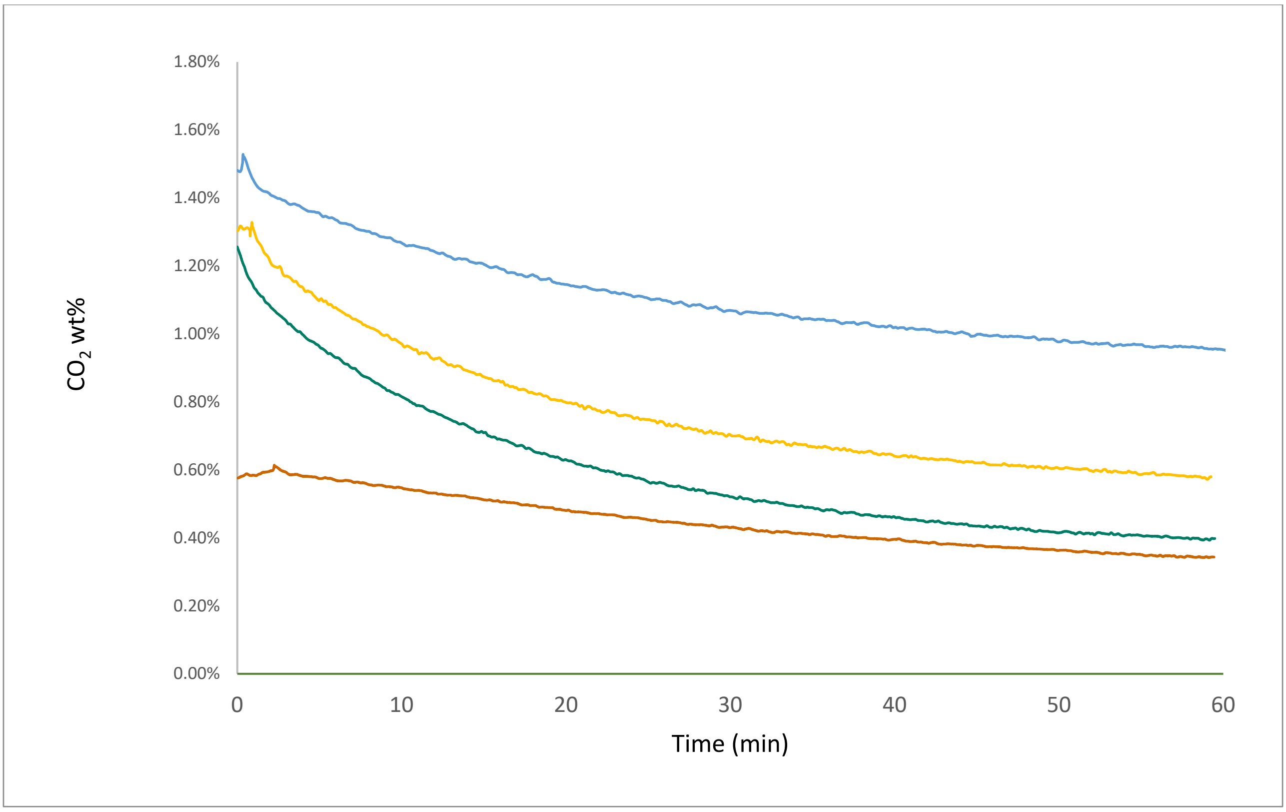

The results show low of CO2 retention following 1 hour of CO2 adsorption. This is likely due in part because of the low capture capacity of these materials at 25 °C and 75 °C. The poor CO2 capture capacity is mainly attributed to the very small surfaces areas of the materials and therefore the grafting methodology does not result in high surface area materials with amine grafted on the surfaces. The CO2 captured at 75 °C is released at a slower rate than for materials that had the adsorption experiment conducted at 25 °C. This suggests that at higher temperatures chemisorption is favoured and results in stable ammonium-carbamate ion pairs which are highly stable and result in slow desorption rates.

Measurement of CO2 release rates on Amine 3 inspired materials

The polymer 1 amine 3 displays CO2 capture capacity of 3.74 wt% at 25 °C and retains only 7 wt% after 1 hour desorption experiment under nitrogen using thermogravimetric analysis (Figure 31). The absence of amine results in fast desorption because the material does not form a mixed carbamate that is stable which ultimately affects the release rates. It was also clear that the materials containing amine 2 had slow rates of CO2 release, even though the capacity was low (<5 wt%).

Figure 31. CO2 desorption of amine inspired materials following 1 hour of CO2 adsorption at 1 bar.1 bar N2 at 80 mL min-1, 25 °C (for 60 minutes). Polymer 1- amine 3 – liq (orange), polymer 1 - amine 3 (blue), polymer 1 amine 3 – amine 2 - (1.5mmol) (green), polymer 1 amine 3 – amine 2 - (1.5mmol) (black).

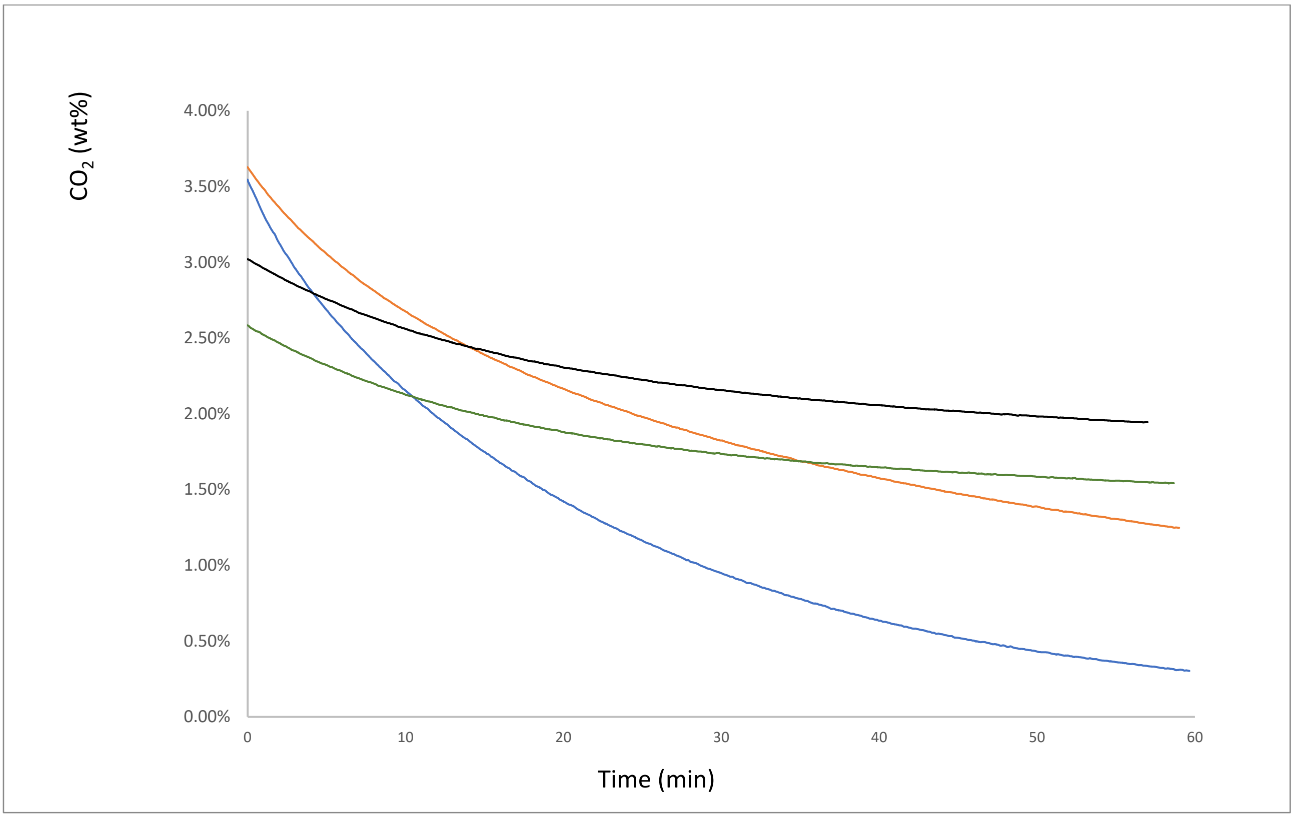

The slow release of CO2 may be attributed to mixed carbamate salt formation which is stable as observed for polymer 1- amine 3 -amine 2 (13wt%), polymer 1 amine 3 -amine 2 (19wt%) and polymer 1 amine 3-liq. After the desorption experiment, the carriers retain 1.95 wt% and 1.54 wt%, which is 56 % and 53 % of the captured CO2 after 1 hour respectively.

The CO2 adsorption and desorption using TGA showed lower capture capacity for the materials, however, with extended exposure to CO2 at elevated temperature (75 degrees) and pressure (10 bar), an improvement in capture capacity was observed (Figure 32, Table 22). This improvement could be due to the high temperature, high pressure and extended reaction times which allows the chemical reaction between amine 3, amine 2 and CO2 to occur to form a mixed carbamate salt. In addition to this improved capacity, the rate of CO2 release was also decreased significantly as shown.

Figure 32. CO2 Desorption at room temperature in air. Polymer 1 – amine 3 – liq (yellow), polymer 1 amine 3 (pink), polymer 1 – amine 3 – amine 2 – 1.5mmol (green), polymer 1 – amine 3 – amine 2 1mmol (blue)

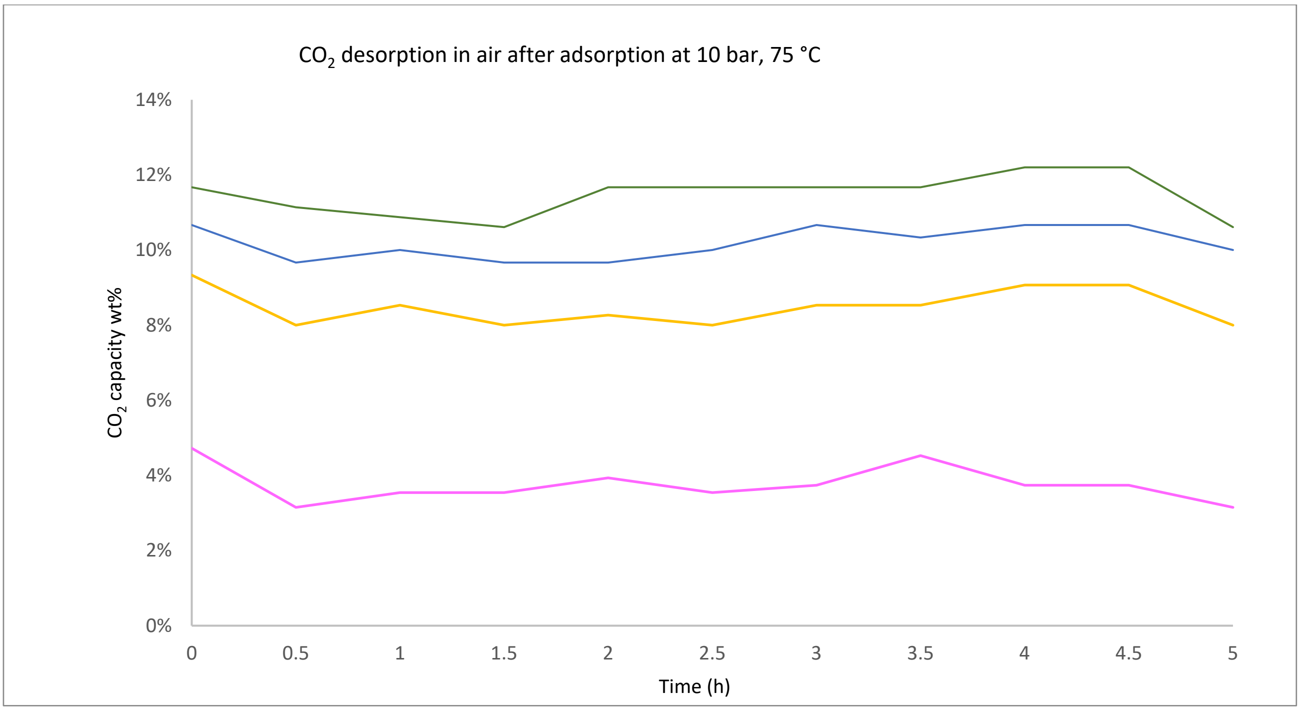

This slow desorption was monitored by taking average weights of the carrier materials exposed to air. Readings were recorded every 30 min for a total of 5 hours. All materials retained the captured CO2 with no significant loss recorded. The samples were left exposed to air overnight and reading taken after 24 h. A significant increase in weight was recorded for all due to absorption of atmospheric moisture over extended periods.

The amine 3 bound polymer displays CO2 capture capacity of 3.74 wt% at 25 °C and retains only 7 wt% after 1 hour desorption experiment under nitrogen using thermogravimetric analysis. The carrier does not form a mixed carbamate as discussed above due to the absence of amine 2 or liquid enhancement. The following reaction occurs.

The material that gave the best capacity is polymer bound amine 2-1.5mmol with a capacity of 11.67 wt% and the amine 2-1 mmol gave a capacity of 10.67 wt%. This polymer 1 amine 3-liquid had a capacity of 9.33 wt% and finally the material without second amine had a capacity of 4.72 wt%. These results show that, the presence of a second amine enhances capture capacity and slows the desorption rates significantly when compared to the TGA results as summarised in table 17.

Table 13. CO_2 desorption rates from TGA and autoclave experiments.

Sample	% CO_2 retained after 1h, 25 °C (TGA)	% CO_2 retained after 1h in air, rt (Autoclave)	% CO_2 retained after 5h in air, rt (Autoclave)
Polymer 1 amine 3	7 %	75.00 %	66.67 %
Polymer 1 amine 3-liq	31 %	91.43 %	85.71 %
Polymer 1 amine 3-amine 2 (13 wt%)	56 %	93.75 %	93.75 %
Polymer bound amine 3-amine 2 (19 wt%)	53 %	93.18 %	90.91 %

Work Package 1.6 – Report on sorbents and identify 3 most promising materials

When summarising the results of the extensive carrier precursor investigation performed in WP1 of this project the following carrier precursors present as the most materials. The most promising materials were selected based upon:

- CO2 capacity: higher CO2 capacities allow for less material usage in cement, meaning less effects on structural properties intrinsic to carrier addition and economic advantages
- Tunability of CO2 release rates and slow CO2 release rates in current iterations.
- Low toxicity/potential for environmental impact
- Greatest flexibility and potential for encapsulation
- amine 2 enhanced silica 1 materials

Despite somewhat moderate CO2 capacities, the covalent grafting of the primary amine-expressing amine 2 group on the surface of silica 1 is particularly promising given the very high CO2 retention and extremely high level of tunability with regards to functionalisation agents and controlling the surface chemistry. Future studies will focus on improving CO2 capacities whilst retaining the slow-release rates and investigations of the CO2 transfer properties in cementitious materials as well as encapsulation technologies to control CO2 desorption rates.

- amine 2 enhanced silica 1/ silica 5 materials

The extremely high CO2 capacity and very slow (~15 wt% at 1 bar) lends the amine 2-enhanced silicas materials to direct trailing in cement as a prospective carrier. The high capacity allows for significant modification which would slightly lower capacity (per unit of mass) whilst retaining a relevant level of CO2 capture. Some tunability comes from the ability to modify the amine used for impregnation. further studies would be initial trails in utilising the amine 2 enhanced silica 1 in cement to observe CO2 transfer, followed by attempts at modifying the CO2 release rates in cementitious environments.

- Polymer 1 amine 3

As a risk-mitigating and valuable alternative strategy the use of polystyrene matrix as a solid backbone to which amine 3/amine 2 and amine 3/amine 1 can be incorporated allows for a broadening of capabilities and interactions in cementitious environments. Exhibiting moderate CO2 capacities and retention rates, significant tunability presents itself through modulating the polymer properties of the polystyrene backbone (molecular weight, crosslinking, hydrodynamic size) and through the trialling of different superbasic materials and complementary amines.